UNIVERSITY OF LEOBEN
DEPARTMENT OF PETROLEUM ENGINEERING
CHAIR FOR DRILLING AND COMPLETION ENGINEERING

VERIFICATION AND COMPARISON OF THE METHODS WHICH USE LOG DATA TO ESTIMATE ROCK PROPERTIES AND INFLUENCE OF ROCK PROPERTIES ON DRILLING DYNAMICS AND BHA DESIGN

MASTER's THESIS

Author:
Žiga Škrjanc, MSc

Supervisor:
Gerhard Thonhauser, Univ.-Prof. Dipl.-Ing. Dr.mont.

Leoben, 2016

PROOF SHEET FOR MSc THESIS SUBMISSION

Name of graduate student: Žiga Škrjanc
Matriculation number: 1435116
Title of the MSc Thesis: Verification and Comparison of the Methods which Use Log Data to Estimate Rock Properties and Influence of Rock Properties on Drilling Dynamics and BHA Design

THE MSc THESIS HAS BEEN SUBMITTED ON ……, ……. .

……..……..

Administration of Montanuniversität Leoben, Main Library

Montanuniversität Leoben, Austria

EIDESSTATTLICHE ERKLÄRUNG

“Ich erkläre an Eides statt, dass ich die vorliegende Diplomarbeit selbständig und ohne fremde Hilfe verfasst, andere als die angegebenen Quellen und Hilfsmittel nicht benutzt und die den benutzten Quellen wörtlich und inhaltlich entnommenen Stellen als solche erkenntlich gemacht habe.“

AFFIDAVIT

“I hereby declare that the content of this work is my own composition and has not been submitted previously for any higher degree. All extracts have been distinguished using quoted references and all information sources have been acknowledged.”

Leoben, _____, 2016

……..

Signature of Graduate Student

Žiga Škrjanc

Acknowledgment

I would like to thank Dipl.-Ing. Dr.mont.Gerhard Pittino, who kindly organized and carried out the UCS tests.

DEDICATION

I dedicate this thesis to my parents who supported me throughout the study.

Kurzfassung

Heutzutage sind Öl- und Gasvorkommen an herausfordernden Orten und in Tiefen, die man vor nur wenigen Jahrzenten gar nicht erreichen konnte. Um diese Lagerstätten zu erreichen, ist modernste Technologie und Know-How erforderlich. Geomechanische Fragen sind nur ein Teil der Herausforderungen bei Bohrungen. Die Auswertung der In-situ-Gesteinseigenschaften ist ein wichtiger Bestandteil der geomechanischen Analyse und es hilft, Prinzipien wie Bohrlochstabilität, Bohrmeißelauswahl, BHA Design, Lochqualität, Steckenbleiben und Bohrungsdynamik. Bohrungsdynamik ist ein weiterer nicht gut durchdrungener Aspekt, der Kosten, NPT und die Zahl der Ausfälle wesentlich erhöhen kann. All dieses Wissen ist entscheidend für eine erfolgreiche Bohrung von gerichteten, stark abgelenkten und horizontalen Bohrlöchern.

Die Arbeit konzentriert sich auf die Modellierung der In-Situ Gesteinsfestigkeit mithilfe akustischer, Dichte- oder anderer Messungen. Für die Arbeit wurden Sandstein- und Kalksteinproben genommen. Aus ihnen wurden Zylinder mit 5 Centimeter Durchmesser gebohrt. Die primäre Wellengeschwindigkeit wurde gemessen und ein UCS-Test (einaxiale Druckfestigkeit) wurde für beide Proben durchgeführt . Als Ergebnis wird der Erfassungsprozess und die empfohlene Verwendung beschrieben.

Bohrungsdynamik kann zu Störungen wie Reibschwingung, niedrige oder hohe Torsionsschwingung, Meißelwirbel oder zufällige Torsionsschwingung führen. Alle diese sind vom BHA Design, Paramatern der Oberflächenbohrung und den Gesteinseigenschaften abhängig. Alle diese Erscheinungen werden in der Arbeit untersucht und als Ergebnis Empfehlungen und beste Bohrpraktiken gegeben.

Abstract

At this present time, oil and gas reservoirs are found in challenging locations and can be reached at depths which were impossible to achieve a few decades ago. In order to reach these reservoirs, both state of the art technology and a great knowledge are required. Geomechanical problems are just one issue which may occur during drilling operations. In situ rock properties evaluation is an important element of geomechanical analysis, which helps in understanding principles such as wellbore stability, bit selection, BHA design, hole quality, stuck pipe studies and drilling dynamics. Drilling dynamics is another phenomenon, which is not well understood and can substantially increase costs, Non-Productive Time ("**NPT**") and failures. All this knowledge is crucial for the successful drilling of directional, highly deviated and horizontal wells.

This thesis focuses on rock strength modelling with the use of logs to enable an estimation of in situ rock properties from sonic, density or another log. Sandstone and limestone rock samples were acquired for this thesis, which were subsequently cored into five centimetre cylinders. Primary wave velocity was measured and a Uniaxial Compressive Strength ("**UCS**") test was carried out on both samples. As a result, the acquiring process is given and recommended usage described.

Drilling dynamics can lead to dysfunctions, such as full stick slip, low or high torsional oscillation, bit whirl or random torsional oscillation. All of these are dependent on BHA design, surface drilling parameters and rock properties. All of these phenomena are investigated in this thesis and, as a result, recommendations and best drilling practices are given.

List of Tables

List of Figures

List of Symbols and Abbreviations

NPT	Non-productive Time
MWD	Measured While Drilling
LWD	Logging While Drilling
BHA	Bottomhole Assembly
GOR	Gas Oil Ratio
M	Molecular weight
V_T	Velocity at temperature T
V_0	Initial velocity
σ_x	Pressure in the x-direction [Pa]
ε_x	Strain in the x-direction [1]
E	Young's modulus [Pa]
v	Poisson's ratio [1]
λ	Lame's first parameter
G	Modulus of rigidity [Pa]
K	Bulk modulus [Pa]
v_p	Primary wave velocity [m/s]
v_s	Secondary wave velocity [m/s]
UCS	Uniaxial Compressive Strength
Δt	Travel time [s] or [µs/ft]
ρ	Density [kg/m^3]
V_{clay}	Clay fraction [1]
ϕ	Porosity [1]
RSS	Rotary Steerable System
HFTO	High Frequency Torsional Oscillation
LFTO	Low Frequency Torsional Oscillation
FSS	Full Stick Slip

Table of contents

1 INTRODUCTION

Wells in the oil and gas industry are becoming increasingly complex and are drilled through formations which were previously unreachable. Due to the nature of such complexity, the risk of various hazards increases and, therefore, more data is needed. One of the challenges is associated with geomechanical evaluation. Issues like wellbore stability, bit selection, BHA design, drilling dynamics and stuck pipe can be affected by a lack of geomechanical data. Specifically, the information is critical for the successful drilling of directional, highly deviated or horizontal wells. During drilling, the data provides the information required to conduct safe operations and to minimise both NPT and trouble time, whilst maximising drilling efficiency.

A lot of time and money are lost due to NPT associated with drilling troubles, which happen due to poor wellbore stability. It is well known that rock properties information increases the effectiveness of drilling and NPT can be significantly reduced if good practices are considered. Due to a lack of geomechanical information, many wells around the world do not reach their planned target depth and have difficulties while drilling, such as stuck pipe, tool failures and wellbore instability (York et al, 2009).

Sonic, resistivity, density or gamma ray logs can be used to estimate in situ mechanical rock properties. These techniques are in use as an alternative to costly and time consuming laboratory tests. The rock properties which are usually determined include UCS, friction angle, cohesion and rock elastic constants, for example, Young's modulus, Poisson's ratio, bulk modulus and shear modulus. This technique has a number of advantages over laboratory measurements (and coring operation) of geomechanical properties, including availability, providing continuous profiles, its low cost and time effectiveness (Odunlami et al., 2011).

Relationships between rocks' physical and mechanical properties were established more than 70 years ago. Wyllie et al. (1956) introduced an empirical relationship between porosity and acoustic velocity of a porous media. The porosity correlation is still widely used today as it gives good results. Many correlations were found in subsequent years, after the introduction. Successful derivation of rock strength based on porosity was conducted on sandstones, carbonates and shales (Sarda et al., 1993, Edlmann et al., 1998, Farquahar et al., 1994, Raaen et al., 1996 and Chang et al., 2006). Rock strength parameters were also determined with the help of Young's modulus (Perkins et al., 1995, Bradford et al., 1998). It was demonstrated that, as porosity increases, elastic moduli, along with UCS, cohesion and angle of internal friction, all decrease (Edlmann et al., 1998, Farquhar et al., 1994).

It is often the case that a sonic log or other logs are unavailable. For example, Santana et al. (2010) developed a correlation between resistivity and sonic log data. The methodology to match these two measurements as accurately as possible was developed and applied on case studies from wells drilled in the Gulf of Mexico.

A new method for estimating in situ mechanical properties from logs was presented in 1996 (Raaen et al.). This method compared the results from more than 200 rock mechanical tests made on cores. The main advantage of this model is that it can be applied to new wells and fields without re-calibration. The authors suggest that a minor calibration can be applied, even though it is not needed. The sensitivity analysis proved that the method is satisfactorily robust.

Odunlami et al. (2011) presented an innovative management platform, where rock parameters were determined exclusively by use of log data. They used all the major empirical methods and concluded that empirical correlations are capable of being used in situations where core data is not readily available. However, local calibration should be completed for a different location. The best correlation gave porosity measurement, as it returned the best estimate of UCS when compared with lab derived core UCS.

Borba et al. (2014) discovered a connection between standard uniaxial test, scratch test and log-based empirical correlation, which were found to be in a good agreement. They suggest that the results can be extrapolated to the entire interval of interest and, furthermore, that the values determined indirectly should be calibrated.

Chang et al. (2006) completed a brief study of different correlation models. The models were evaluated and a large set of data was used to calculate and compare results with physical property data from the literature. It was concluded that some equations work reasonably well, whereas individual rock strength variations with individual physical properties scatter considerably. Therefore, local calibration is suggested.

When the rock properties are defined, an evaluation of other operational phenomena can begin, such as drilling dynamics, which is the logical continuation once the rock properties are obtained with the help of the empirical correlations described above. Drilling dynamics is defined as being all of the dynamic movements of the drill string, which occur at certain frequencies due to an applied load, or interaction between two elements (for example, the drill string and the wall). In this thesis, special focus will be given on the BHA drilling dynamics, how the dynamics are affected by rock properties (especially UCS) and the resultant effect on drilling operations.

A great deal of research has been carried out on drilling dynamics, the severe behaviour of which forced oil companies to seek to prevent the problem, with many failures being reported in the literature. MWD tools, roller reamers, joints, LWD and other tools failed due to drilling dynamics dysfunctions (Payne, 1992, Chen, 2007, Mason, 1998, Chatar et al., 2011, Ramizer et al., 2010, Bailey et al., 2009).

In addition, to change operating parameters and introduce real time monitoring, a proper planning and BHA design should be prepared to prevent drilling dynamics dysfunctions. The most common phenomena are BHA whirl and stick-slip, which can occur as a result of torsional movements, bit bounce and torsional accelerations. All these effects can contribute to significant NPT which, consequently, increases both the drilling time and costs of the well. After taking proper steps to mitigate or eliminate these dysfunctions, NPT decreased up to 40% in some cases (Bailey et al., 2009, Burgess et al., 1987, Reckmann et al., 2010).

It was difficult to evaluate the drilling dynamics until the proper measurement devices appeared. It had previously been thought that high frequency vibrations did not damage either the tools or the wellbore. It was later discovered, with the help of high frequency measurements, that they can cause significant and severe excitations which may lead to tools failure (Oueslati et al., 2013). Therefore, at present, all the frequencies are measured, in order to get a full picture of drilling dynamics.

The thesis objectives

Several objectives are set for the thesis. Most of the correlations found in the literature are stated in the thesis. Additionally, limestone correlations from Farquhar et al. (1994), Militzer (1973), Golubev (1973) and Chang et al. (2006) and sandstone correlations from Freyburg (1972), Vernik et al. (1993), Farquhar et al. (1994), Sarda et al. (1993), Raeen et al. (1996), Moor et al. (1999), Rahman et al. (2010), and Chang et al. (2006) are used in order to meet the following objectives:

1. Comparison of the correlations above with an experiment in which a sandstone and limestone samples are tested. Sonic velocity, porosity and UCS values are measured on both samples. As a result, the sonic velocity and porosity values are used in the correlations and compared to the UCS values obtained in a laboratory.
2. Usage of the empirical correlations is verified, including their impact on cost – effectivness, time savings and information quality.
3. Derivation of recommended procedures how to use the empirical correlations in a new field.

Drilling dynamics is an important phenomenon, which occurs during drilling operations and its knowledge can help with drilling the well on time, reduce NPT and hit the target. Drilling

dynamics is dependent on rock properties. Therefore, the relationship between them is studied in the thesis with the following objectives set:

1. How a formation dip affects drilling dynamics.
2. Influence of friction factor on BHA vibrations.
3. Drilling dynamics response to hard rocks (high UCS) stringers within a soft and loose formation.

2 THEORY AND BASICS

2.1 ROCK PROPERTIES

2.1.1 Introduction

Because the thesis is dealing with rock properties and their effect on BHA design and drilling dynamics, this chapter will provide some theory about them. General rock properties will be described and the most common rocks which appear in the oil and gas industry discussed.

Rocks are defined as aggregates of minerals plus pore space which can be empty or filled with a fluid. In general, the three major rock types are classified as igneous, metamorphic and sedimentary. (Lake, 2007)

Minerals have definite structure, composition and properties which are dependent on their chemistry and structure. There are hundreds of minerals in the Earth's crust but in the oil and gas industry we usually deal with rather low number of them. They can be broken into silicates, sulphates, sulphides, carbonates, and oxides. Often, organic compounds such as coal or bitumen are present. Classification can be further broken into the most common used elements in the oil and gas industry (Lake, 2007):

- Common silicates:
  - Quartz.
  - Feldspars.
  - Micas.
  - Zeolites.
  - Clays.
- Common carbonates:
  - Calcite
  - Dolomite
  - Siderite may be present.
- Oxides:
  - Magnetite
  - Hematite

Usually, the knowledge about quartz, feldspars, clays, calcite, dolomite and anhydrite is enough to fulfil most engineering needs.

One of the most problematic minerals and the least understood are clays. They are problematic because their properties change significantly with in-situ pressure, temperature and chemical environment. Parts of clays can be presented in other rocks, for instance in sandstone, which makes the understanding about rocks behaviour significantly more difficult. (Lake, 2007)

2.1.2 Density and porosity

Density and porosity are one of the most important parameters, which further affect properties such as the strength, acoustic velocities, elasticity and others. Density of rocks is more complex because of many phases presented inside the void spaces.

The basic definition of density is mass per volume. For homogeneous or single-phase material, the definition of density is simple. However, rocks are usually mixtures of several phases, both solids and fluids.

Porosity directly affects density because a fluid is always present in pores. It is defined as the nonsolid or pore-volume fraction. It is worth mentioning different volumes, which are often used. For instance, total volume of rock, volume of mineral phase, volume of pores or openings, volume of interconnected pores, volume of isolated pores, volume of cracks or fractures and volume of different fluid phases. From these we can define the various kinds of porosity such as total porosity, effective porosity, ineffective porosity and crack or fracture porosity.

The figure below shows how porosity is dependent on density and vice-versa.

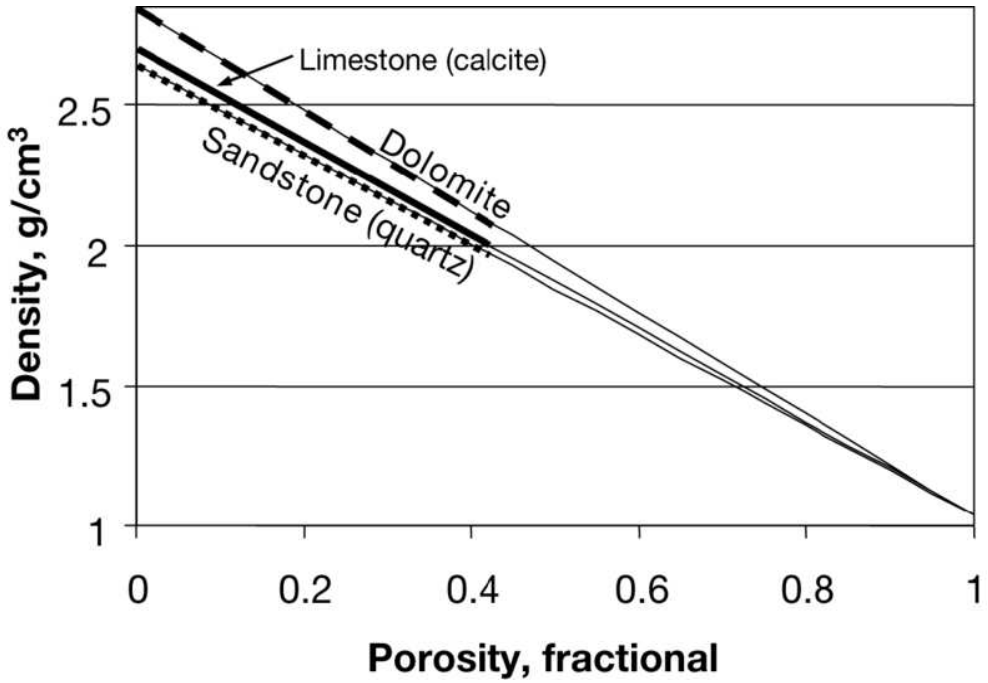

Figure 1: Density vs. porosity for limestone, dolomite and sandstone. (Lake, 2007)

Generally, density increases and porosity decreases with depth. It is clear, that this happens because differential pressures usually increase with depth. As pressure increases, grains reach a more dense packing. However, that might not be the case at all times because differential or effective pressures do not always increase with increasing depth. Abnormally high pore fluid pressures can occur. The high pore pressure results in an abnormally low differential of effective pressure, which can retard or even reverse the normal compaction trends. (Lake, 2007)

Porosity effect on acoustic properties

Porosity directly affects acoustic properties of a rock. It is known that two acoustic limits exist. First, the upper limit or Voigt limit and second, Reuss limit or the lower limit. The velocity is within the range of the two limits (Hashin et al., 1963). The Reuss lower bound is sometimes called the isostress average because it gives the ratio of average stress to average strain when all constituents are assumed to have the same stress (Mavko et al., 1998).

There is often a great difference between these idealized bounds and real rocks. Some dolomites might reach Voigt limit. Typically, we should begin with a mineral velocity and then decrease it with increasing porosity. This is true until certain extend because at high porosities, grains separate and the mixture acts as a suspension. This limit is usually called critical porosity. (Lake, 2007 after Yin et al. and Nur et al.)

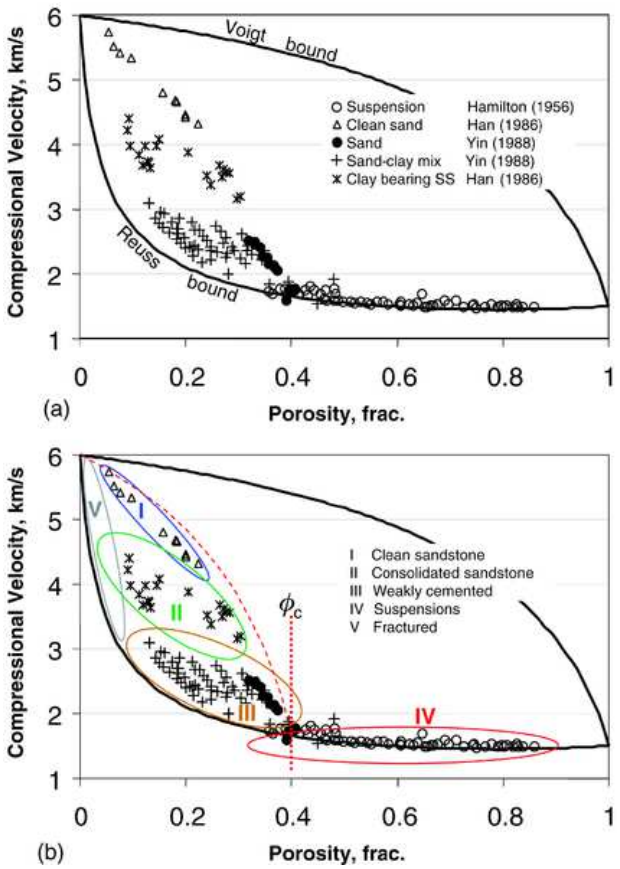

Figure 2: Dependence of compressional velocity on porosity for different rocks. (Lake, 2007)

Additionally, one should take care about critical porosity values. The critical porosity means, that when it is reached it separates mechanical and acoustic behaviour into two distinct domains. For porosities lower than critical porosity, the mineral grains are still capable to be loaded, whereas for porosities greater than critical porosity the rock falls apart and becomes a suspension in which the fluid phase is load-bearing. It is clear, that above this porosity the acoustic measurements will not work. Therefore, special care should be taken about this. Some typical values of critical porosities are shown in the table below (Mavko et al., 1998):

Table 1: Typical values of critical porosity. (Mavko et al., 1998)

Material	Critical Porosity
Sandstones	40%
Limestones	60%
Dolomites	40%
Chalks	65%
Rock salt	40%
Cracked igneous rocks	5%

2.1.3 Fluid properties – acoustic

Rocks consist of pores and they can contain different fluids. The fluid inside the pores could be water, air, oil or gas. The properties of fluids are needed if we wish to interpret the laboratory data or in-situ data from logs or seismic measurements. Logging tools are greatly affected by acoustic properties of a fluid, which is in the pores. The fluid acoustic properties are dependent on temperature, pressure, overburden stress and others. The same fluid could behave differently under different circumstances.

Oil

The oil itself has already different properties – it can be a heavy or very light oil. Because of its properties the oil can transform from liquid phase to a quasi-solid phase with drastic increase of viscosity. Therefore, P-wave velocity and S-wave velocity change drastically. In some cases the velocity can change up to 50%. It is clear that a fluids composition should be evaluated carefully. Additionally, the velocities are highly dependent on GOR (Gas-Oil Ratio), temperature and pressure of the oil. (Han et al., 2006)

It is a well-known fact that sound velocity depends on media. In the air, the speed of sound is 1.236 km/h. In water the speed increases for more than four times, up to 5.342 km/h and in solids like rocks or metals the speed is the highest. Please note that the speeds stated before are in ideal conditions. Like stated before the velocity can change significantly when temperature or pressure changes. A problem which may arise when dealing with different fluids is that the composition of the fluid is rarely known.

Many correlations describe how moduli typically increases with increasing temperature and increases with increasing pressure. Wang and Nur (1998) did an extensive study of several hydrocarbons and found simple relationships among the density, moduli, temperature and carbon number (Lake, 2007):

$$V_T = V_0 - b\Delta T \tag{1}$$

where V_0 is the initial velocity, V_T is the velocity at temperature T, ΔT is the temperature change, and b is a constant for each compound of molecular weight M:

$$b = 0.306 - 7.6/M \tag{2}$$

Similarly, the velocities are related in molecular weight by:

$$V_{TM} = V_{TOMO} - b\Delta T - a_m[\frac{1}{M} - \frac{1}{M_0}] \quad (3)$$

where V_{TM} is the velocity of oil of weight M, and V_{TOMO} is the velocity of a reference oil of weight M_0 at temperature T_0. The variable a_m is a positive function of temperature. It is clearly visible that the velocity of the fluid will increase with increasing molecular weight. However, more complex compositions can occur and the influence of pressure should be considered as well.

For predicting the frequency-dependent velocities of saturated rocks in terms of the dry rock properties, formulas were derived by Biot (1956). The formulas incorporate some of the mechanisms of viscous and inertial interaction between the pore fluid and the mineral matrix of the rock. The formulas are based on the limiting velocities which are the same as predicted by Gassmann's relations (Mavko et al., 1998).

Brines

The most common fluid during drilling through different rock masses consist of brines. Their composition can range from pure water to saturated saline solutions. The concentration of brines can vary from field to field. Salinity of brines is an important parameter because it obviously increases their density. Many correlations to calculate density of a brine were developed. Due to different density of brines the sound velocity can greatly differ from brine to brine. (Lake, 2007)

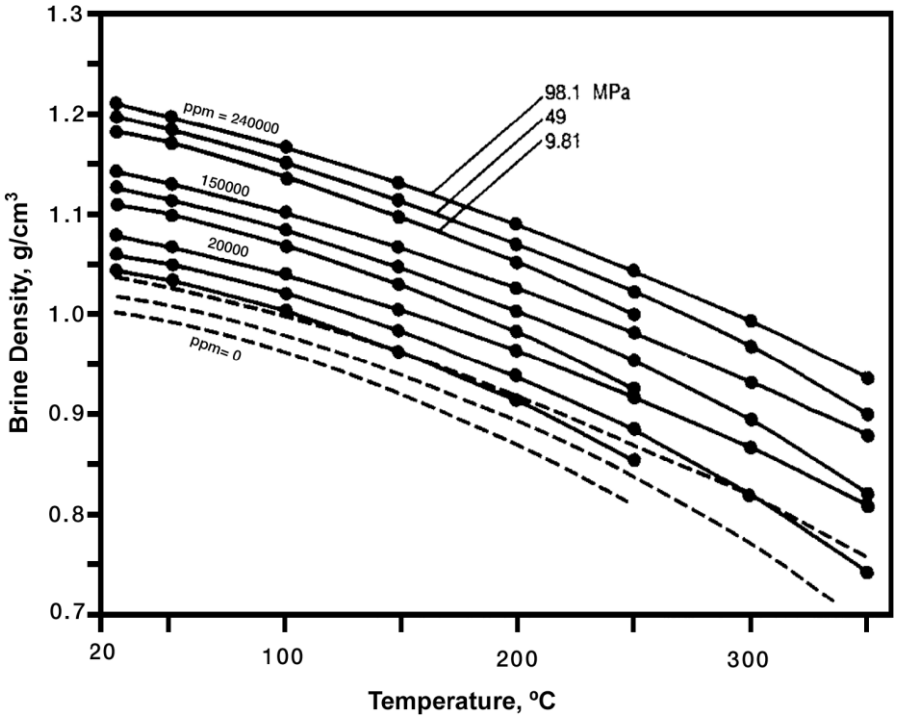

Figure 3: The dependance of brine density on temperature and salinity content in ppm. (Lake, 2007)

2.1.4 Elastic moduli

In the previous chapter some basic properties were described. Because we deal with rocks, some elastic properties are important. The most important will be listed and briefly described in this chapter. The parameters described here, will be later used for the experiments and analyses.

The theory of linear elasticity deals with situations where there are linear relationships between applied stresses and resulting strains. While most rocks do behave nonlinearly when subject to large stresses, their behaviour may normally be described by linear relations for sufficiently small changes in stress. For instance, consider a sample of length L and cross-sectional area $A = D^2$. When the force F is applied, the corresponding length of the sample is reduced to L′. The applied stress is then $\sigma_x = F/A$ and the elongation is $\varepsilon_x = (L - L')/L$. If the sample behaves linearly, there is a linear relation between σ_x and ε_x, which we can write as (Fjaer et al., 2008):

$$\varepsilon_x = \frac{1}{E}\sigma_x \tag{4}$$

The equation above is known as Hooke's law, while the coefficient E is called Young's modulus. This modulus is the first one of elastic moduli coefficients. Young's modulus is actually a measure of the stiffness of the sample, in other words, the sample's resistance

against being compressed by the uniaxial stress (Fjaer et al., 2008). A perfectly rigid material has an infinite Young's modulus, because an infinite force is needed to deform such a material. Therefore, it can be said that material which has a high Young's modulus is approximated as rigid.

If a stress is applied, there will be another consequence; an increase in width D of the sample. The lateral elongation is defined as $\varepsilon_y = \varepsilon_z = (D - D')/D$. The ratio between axial and lateral elongations is defined as:

$$v = -\frac{\varepsilon_y}{\varepsilon_x} \tag{5}$$

This is another important elastic parameter, known as Poisson's ratio. It is a measure of lateral expansion relative to longitudinal contraction. Most materials have Poisson's ratio between 0.0 and 0.5. If the material is ideally incompressible at small strains, then the material would have Poisson's ratio of exactly 0.5. On the contrary, a material which shows little lateral expansion when compressed would have Poisson's ratio of 0, such as unconsolidated sands. There are some materials which can reach the negative ratio, for instance, weak porous rocks. Typically, for rocks Poisson's ratio is between 0.15 – 0.25.

Another important elastic moduli are λ and G. They are known as Lame's parameters. Sometimes, they are called Lame's first parameter and Lame's second parameter, respectively. Alternatively, G is known as modulus of rigidity, or the shear modulus. This means that it measures the material's resistance against shear deformation. The shear modulus is also important in acoustic of rocks, because the shear wave velocity is directly dependent on it.

Table 2: Some relations between elastic moduli. (Fjaer et al., 2008)

$\boldsymbol{E = 3K(1 - 2v)}$	$\boldsymbol{K = \lambda\frac{1+v}{3v}}$	$\boldsymbol{2v = \frac{\lambda}{\lambda + G}}$
$\boldsymbol{E = 2G(1 + v)}$	$K = \frac{2}{3}G\frac{1+v}{1-2v}$	$\frac{G}{\lambda + G} = 1 - 2v$
$\boldsymbol{E = \frac{9KG}{3K + G}}$	$K = \lambda + \frac{2}{3}G$	$\frac{\lambda + 2G}{\lambda + G} = 2(1 - v)$
$\boldsymbol{E = G\frac{3\,\lambda + 2G}{\lambda + G}}$	$K = \frac{GE}{9G - 3E}$	$\frac{3\lambda + 2G}{\lambda + G} = 2(1 + v)$
$\boldsymbol{E = \frac{\lambda}{v}(1 + v)(1 - 2v)}$	$\frac{\lambda}{G} = \frac{2v}{1-2v}$	$v = \frac{3K - 2G}{2(3K + G)}$
$\boldsymbol{H = \lambda + 2G}$		

Bulk modulus is another important elastic modulus. It is defined as the ratio of hydrostatic stress σ_p relative to the volumetric strain ε_{vol} (Fjaer et al., 2008). It can be written as:

$$K = \frac{\sigma_p}{\varepsilon_{vol}} = \lambda + \frac{2}{3}G \tag{6}$$

As it can be seen, K is the measure of the material's resistance against hydrostatic compression. The inverse of K, 1/K is known as compressibility. Some typical values of bulk modulus for materials can be seen in the table below:

Table 3 Typical bulk modulus values for the most common materials.

Material	Bulk modulus in Pa
Water	2.2×10^9
Air	1.42×10^5
Steel	160×10^9
Diamond	443×10^9
Quartz	36.4×10^9

Interestingly, if any two of moduli E, v, λ or K are defined, the remaining ones can be calculated with a help of correlations, as seen in Table 2.

Modulus H which is defined as uniaxial compaction modulus or oedometer modulus, is also important. It is mentioned here because it is crucial in terms of acoustic; it is referred as the plane wave modulus or P-wave modulus.

2.1.5 P- and S- waves

In acoustics, two waves usually occur: P- and S- waves. A P-wave is also called longitudinal, or alternatively compressional wave because it involves a periodic compression of the material. In the literature, it can be named as a primary wave, a name which originates from studies of earthquakes. If we consider a typical X,Y coordinate system, the P- wave moves particles of the material and it is propagating in X- direction. On the contrary, the S- wave is a wave which moves the particles in Y- direction but it propagates in X- direction. Because of that, the wave is often called a transversal wave, shear wave, or secondary wave. Interestingly, a well-known fact is that primary wave is always larger than secondary wave in an isotropic, linearly elastic solid. (Fjaer et al., 2008)

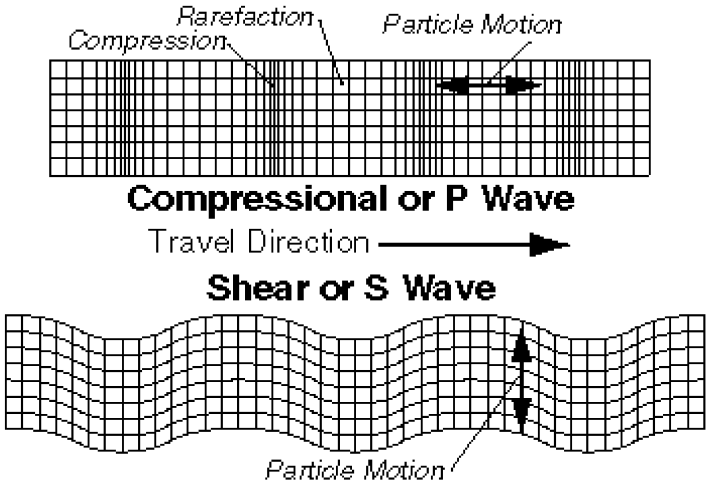

Figure 4: Schematic of the compressional wave and secondary wave. (www.colorado.edu)

Interestingly, all the terms in Table 1 can be expressed with acoustic velocities. For instance, Lame's parameters can be expressed as:

$$G = \rho {v_s}^2 \tag{7}$$

$$\lambda = \rho v_p^2 - 2\rho v_s^2 \tag{8}$$

Furthermore, these correlations can be expanded with a help of Table 1:

$$K = \rho v_p^2 - \frac{4}{3}\rho v_s^2 \tag{9}$$

$$E = \rho v_s^2 \frac{3v_p^2 - 4v_s^2}{v_p^2 - v_s^2} \tag{10}$$

$$v = \frac{v_p^2 - 2v_s^2}{2(v_p^2 - v_s^2)} \tag{11}$$

It is important to know, that these relations are valid only for a linearly elastic, isotropic and homogenous material. Because rocks are usually neither isotropic nor homogenous, nor are they linearly elastic, the issues will be discussed in the next chapter.

2.1.6 Issues related to acoustic measurements relations

As seen in the previous chapter, elastic moduli can be easily derived from acoustic measurements. If it is so easy, a question arises why empirical correlations for rocks were developed and why these properties are still measured with a classic uniaxial tests. The problem is, that, in reality, rocks are not homogenous, neither isotropic nor linearly elastic. Moreover, the porosity of rocks make it even more complex.

There is a wide range of literature showing that the elastic moduli obtained from a usual rock mechanical test (which are called static moduli) differ significantly from those obtained with acoustic velocities (which are called dynamic moduli). The evidence shows, that normally, the dynamic moduli are larger than static moduli. The difference is usually larger for weak rocks. (Fjaer et al., 2008)

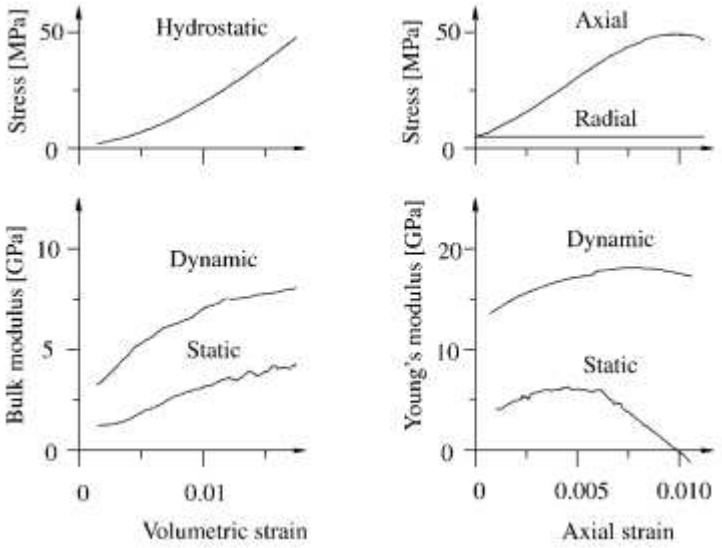

Figure 5: Static and dynamic bulk moduli as measured during a hydrostatic test (left) and static and dynamic moduli as measured during a triaxial test (right). (Fjaer et al., 2008)

As mentioned before, one of the reasons is porosity. There is usually a fluid in the pores which can significantly change the velocities. Fjaer et al. (2008), argue that velocity dispersion due to fluid saturation is in ranges of a few percent from seismic to ultrasonic frequencies. Thus, this cannot be the reason for such a big difference.

During a velocity measurement, the strain rate is at either ultrasonic frequencies or seismic frequencies, at 10^{-1} s^{-1} and 10^{-4} s^{-1}, respectively while the strain amplitude is usually between 10^{-7} and 10^{-6} s^{-1}. However, the strain rate for a static measurement is usually lower than 10^{-2} s^{-1} and the strain amplitude is usually between 10^{-2} and 10^{-3}. Hence, the major difference between static and dynamic measurements is the strain amplitude which differs because of plasticity or nonlinear effects (Fjaer et al., 2008).

To understand rocks behaviour, other materials' behaviour should be checked first. It is interesting to notice, that the static and dynamic are equal for homogeneous, elastic material like steel. If we know that, it can be said that the physical origin of this discrepancy is most likely related to heterogeneous microstructure of rocks (Ledbetter, 1993). Furthermore, the

effect originates mostly at the grain contacts, since the stress concentration there may exceed the elasticity limit of the material even when the external stress is low.

Stress history of rocks is also an important parameter for sound velocities. A side effect of different stresses is also change in porosity and therefore density of the material. But this is not the main reason for a major change. The behaviour can be understood as in terms of micro-cracks which are smaller than the wavelength and are opened or closed by the action of the stress. It is clear, that an open crack strongly reduces the velocity of a wave if the crack is oriented normal to the direction of propagation of the wave, while its effect is not so significant other way around (Fjaer et al., 2008).

When an elastic wave hits a boundary of the medium it is travelling through, the wave may be reflected, refracted or converted into other types of elastic waves. Such boundaries are very important for acoustics measurements. Actually, the principle of reflection is the foundation for surface seismics and refraction is the foundation for sonic logging tools. What can often happen is so-called polarization. This is when the symmetry between the waves is broken and they become coupled at the interface.

The description above sum up how some properties affect acoustic measurements and elastic moduli. Anyways, there is one more effect which was skipped: chemical effects. Especially, the minerals in the rock may react with pore fluid. This is especially true for chalk and clay minerals which are highly sensitive. It means that fluid substitution may actually change the framework moduli. Hence the elastic wave velocities, as well as the static elastic moduli are very sensitive to the type of saturating fluid. (Fjaer et al., 2008)

2.1.7 General mechanical behaviour of rocks

A lot of research has been done on this topic and many triaxial tests have been done to better understand rocks behaviour. Even in the earliest experiments on rocks, it was recognized that rock strength increases with increasing confining pressure (overburden pressure).

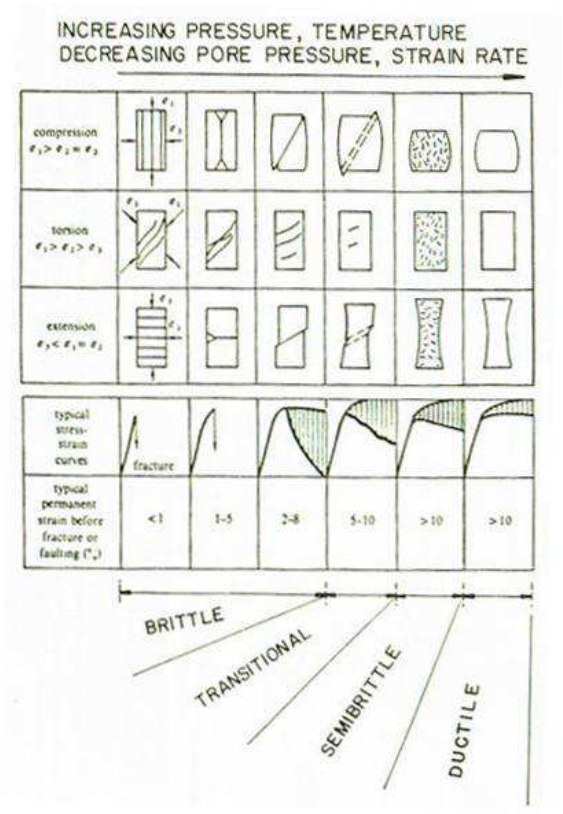

Figure 6: Schenatic representation of the influences of environmental paramaters on the macroscopic behaviour, stress-strain relations, and ductility of rocks in triaxial tests. (Carmichael, 1990)

Generally, three rock behaviours are known: brittle, semi-brittle and ductile regime. In brittle regime displacements and strains are localized along discrete surfaces (fractures or faults). At the lowest pressures, extension fractures (axial splitting in compression tests) occur in orientations perpendicular to the least principle stress. Failure occurs because of local tensile stress. When the pressure increases, rocks do not break perpendicularly anymore, but usually in range from 10 – 35°. If temperature increases with pressure, then loss of cohesion does not accompany the localization of strain along shear surfaces; this process is called faulting. (Carmichael, 1990)

Semi-brittle regime occurs when macroscopic strains due to stable microfracturing and to the mechanisms of crystal plasticity are distributed throughout the rock. Large increases in volume typically are associated with the microfracturing in low porosity rocks and strains exceeding twenty percent can be sustained without fracture or faulting. Strength increases nonlinearly with increasing confining pressure and increasing confining pressure. (Carmichael, 1990)

Ductile regime occurs when confining pressure is even higher. Microfracturing is actually suppressed and the mechanisms of plastic glide (slip, twinning, and transformation glide)

dominate at low to intermediate temperatures. The slope of the stress-strain curve is insensitive to changes in confining pressure. (Carmichael, 1990)

2.2 LOG DERIVATIVE METHODS

All the available correlations which can be found in literature will be given and listed in this chapter. They are developed mainly for sandstones, carbonates (limestone, dolomite) and shales. Therefore, they are split into three categories. Furthermore, they are derived from either porosity, travel time and sonic speed or Young's modulus. These correlations will be later on applied on the real samples in the chapter "experiments".

2.2.1 Determination of sandstone rock properties

2.2.1.1 Strength as a function of porosity for sandstone

According to Vernik et al (1993) porosity was identified as the best predictor of rock strength in sedimentary rocks. The research included 52 cores of carbonate poor siliciclastic rocks from a broad range of sedimentary basins on which 195 drained, compressive triaxial tests were conducted including 27 unconfined tests. The porosities varied between 1% and 36%. They classified the core samples into arenites and clean arenites (volume of clay less 3% and 3-15%, respectively) and derived the following empirical correlation (Odunlami et al., 2011):

$$UCS = 254 \times (1 - 0.027\phi)^2 \tag{12}$$

where UCS is in MPa and ϕ is in percentage. The equation has been claimed to have a global application for sandstones.

Edlmann et al. (1998) claimed that porosity gives a better continuous representation and a wider scope rock properties than acoustic data. Therefore, they were focused on finding relationships between log-derived porosity and rock mechanical properties. Additionally, they stated empirical correlations between porosity and other rock properties such as elastic moduli, strength moduli, cohesion, angle of internal friction, Poisson's ratio and stress factor. For uniaxial compressive strength (UCS) the following correlation was found:

$$UCS = -3.225\phi + 129.54 \tag{13}$$

where UCS is in MPa and ϕ is in percentage. Authors claim that the correlation can be applied on a wide range of sandstones.

Farquhar et al. (1994) determined another set of correlations for sandstones and carbonates. UCS, static and dynamic elastic modules were determined. They claim that the correlation should be used with caution, because they provide an estimate of the mechanical properties when core material is not available for testing. The correlation of UCS for sandstones is as follows:

$$UCS = 208.08 \times e^{0.074\,\phi} \tag{14}$$

where UCS is in MPa and ϕ is in percentage.

Sarda et al. (1993) evaluated compressive strength based on logs from a well on Germigny-sous-Coulombs structure. The relationships between compressive strength and porosity were developed using a theoretical approach of grain contacts, the analysis of published rock mechanics data and mechanical measurements on plugs taken from well cores. The relationships were primarily found to prevent sand production. The correlations were found for a set of porosities:

$$0 < \phi < 0.07 \qquad UCS = 357 \times e^{-10.8\,\phi} \tag{15}$$

$$0.07 < \phi < 0.3 \qquad UCS = 258 \times e^{-9.0\,\phi} \tag{16}$$

$$0.3 < \phi \qquad UCS = 115 \times e^{-11.6\,\phi} \tag{17}$$

where UCS is in MPa and ϕ is in percentage. The correlations were found on many different types of sandstone.

Raaen et al. (1996) developed an alternate method for estimating in situ rock properties from logs. The model is based on processes which occur in rocks during mechanical loading. They focused on the mechanisms which give rise to differences between static and dynamic elastic moduli. These mechanisms were included into their model. Afterwards, they compared the results with data from laboratory tests on 235 core samples from several fields in the North Sea and mid-Norway. A correlation coefficient of 0.88 was achieved and following correlation found:

$$UCS = 43 - 140\,\phi + 63\,\phi^2 \tag{18}$$

where UCS is in MPa and ϕ is in percentage. The equation should be only used for porosities in a range from 0.2 to 0.35.

Chang et al. (2006) developed a correlation for carbonates. They did not state for which area the correlation works the best, but it can be assumed that it is applicable worldwide. It works the best for sandstones with UCS between 2 and 360 MPa, with porosity between 0.002 and 0.33.

$$UCS = 277\, e^{-10\,\phi} \tag{19}$$

Where UCS is in MPa and ϕ is in fraction.

2.2.1.2 Strength as a function of sonic velocity or travel time

In the literature review of Chang et al. (2006) a correlation for sandstones in Thuringia region, Germany can be found. The correlation was developed by Freyburg (1972):

$$UCS = 0.035\, V_p - 31.5 \tag{20}$$

Where UCS is in MPa nad V_p is in m/s.

Raaen et al. (1996) developed a method for in situ properties of sandstones. The method is based on compressional sonic log. They claim that it works the best for estimating strength at non-zero confining stress and for porosities under 35%. Additionally, the validity range of travel time is between 90 and 140 µs/ft. The equation is as follows:

$$UCS = 140 - 2.1\Delta t + 0.0083\Delta t^2 \tag{21}$$

Where UCS is in MPa and Δt is in µs/ft.

In order to prevent open hole interval of a wellbore within the Hemlock Sands of the McArthur River Field, Cook Inlet, Alaska, Moor et al. (1999) developed a correlation for UCS estimation. They found out that the relationship for the fine-grained sands was indistinguishable from that for the medium- and coarse-grained sands, and therefore a single correlation was used:

$$UCS = 1.745 \times 10^{-9} \times \rho \times {V_p}^2 - 21 \tag{22}$$

Where UCS is in MPa, ρ is density in g/cc and V_p is in m/s. A caution should be taken when use the correlation because it was used only for clean sandstones and is therefore not applicable to other lithologies.

Rahman et al. (2010) proposed a correlation for sandstones in a reservoir in South East Asia. The correlation was used to prevent sand production from a gas reservoir. The rock strengths values were derived from multi-stage triaxial tests and correlated with corresponding sonic travel time:

$$UCS = 40847 \times e^{-0.0268\Delta t} \tag{23}$$

Where UCS is in psi and Δt is in µs/ft.

Likewise, Chang et al. (2006) proposed their own correlation after evaluating more than 260 models for sandstones:

$$UCS = 42{,}1\ e^{1.9\times10^{-11}\rho V_p^2} \tag{24}$$

Where UCS is in MPa, ρ is in kg/m^3 and V_p is in m/s.

2.2.1.3 Strength as a function of Young's modulus

According to the literature review, Young's modulus provides the best estimate for rock strength when the rocks are clastic with large differences in clay content and porosity. This is due to the fact that Young's modulus is a measure of rockc matrix which actually bears the load, and is correlated with the geometry and average number of gran to grain contacts. (Odunlami 2011 after Plumb 1994)

Often, the best information about rock parameters is not static Young's modulus but dynamic one. If dynamic Young's modulus is known, then rock strength can be calculated with a help of correlation developed by Plumb (1994):

$$UCS = 2.28 + 0.007(E_{dyn})^2 \tag{25}$$

where UCS is in psi and E_{dyn} is in GPa.

Perkins et al. (1995) took samples from 13 fields in the U.S. Gulf Coast area and developed a correlation with a help of Young's modulus:

$$UCS = 10^{-12}(114 + 97\ V_{clay}) \times K_b \times E_{dyn} \tag{26}$$

where UCS is in psi, E_{dyn} and K_b are in Gpa and V_{clay} is in fraction.

Chang et al. (2006) also found a correlation between Young's modulus and UCS:

$$UCS = (46.2 \times e^{0.027*E}) \times 145 \tag{27}$$

where E is Young's modulus in MPa and UCS is in MPa.

2.2.2 Correlations for carbonates

2.2.2.1 Strength as a function of porosity

Farquhar et al. (1994) developed a relationship between porosity and rock strength for carbonates. The rock samples were from a wide range of reservoirs in the North Sea. The following correlation was derived:

$$UCS = 174.80 \times e^{0.093\,\phi} \tag{28}$$

Where UCS is in MPa and ϕ is in fraction.

2.2.2.2 Rock Strength as a function of Sonic Velocity/Travel Time

As for others, Chang et al. (2006) developed a correlation between travel time and rock strength:

$$UCS = 145 \times 1.4138 \times 10^7 \times \Delta t^{-3} \tag{29}$$

Where UCS is in MPa and is in µs/ft.
In the paper of Chang et al. (2006) a few other correlations were presented which were developed by Golubev (1976) and Militzer (1973). They use sonic velocity time to calculate rock strength.

$$UCS = \frac{10^{2.44+\frac{109.14}{\Delta t}}}{145} \text{ (Golubev)} \tag{30}$$

$$UCS = \frac{\left(\frac{7682}{\Delta t}\right)^{1.82}}{145} \text{ (Militzer)} \tag{31}$$

Where UCS is in MPa and Δt is in µs/ft.

2.2.3 Correlations for shales

Although, shale sections are rarely cored their properties are still important for drilling operations. They greatly influence wellbore stability, rate of penetration, drilling dynamics and BHA design.

Horsurd (2001) analysed many cores from the North Sea and the Norwegian Continental Shelf in order to determine rock strength in shale as a function of porosity. With a correlation coefficient of 0.98 he found the correlation:

$$UCS = 243.6 \times \phi^{-0.96} \tag{32}$$

Likewise, Horsurd (2001) found a good correlation between laboratory measured P-wave velocity and rock strength with a correlation coefficient of 0.99. The correlation was made in laboratory which could lead to a big error when used in the field, because shales are prone to temperature effects. The equation is as follows:

$$UCS = 0.77 \times \left(\frac{304.8}{\Delta t}\right)^{2.93} \tag{33}$$

Where UCS is in MPa, ϕ is in fraction and Δt is in μs/ft.

Additionally, Horsurd (2001) developed a correlation between Young's modulus and rock strength:

$$UCS = 8.03\ E^{0.91} \tag{34}$$

Where UCS is in MPa and E is in GPa.

2.3 V_P – V_S RELATIONS

V_P – V_S are the most important parameters when determining a lithology from seismic or sonic log data. For the correlations in the previous chapter, it is usually preferred to know the lithology. Therefore, a few relations will be described in this chapter.

Limestones

Many laboratory $V_P - V_S$ correlations for water-saturated limestones were made by Pickett (1963), Milholland et al. (1980), and Castagna et al. (1993). Castagna et al. (1993) compared them with Pickett's (1963) correlations which is derived from laboratory core data (Mavko et al., 1998):

$$V_S = V_P/1.9 \tag{35}$$

And a least-squares polynomial fit to the data derived by Castagna et al. (1993):

$$V_S = -0.055\,V_P^2 + 1.017V_P - 1.031 \tag{36}$$

The Pickett's correlation fits better at higher velocities, but in any case, the second correlations is recommended to use.

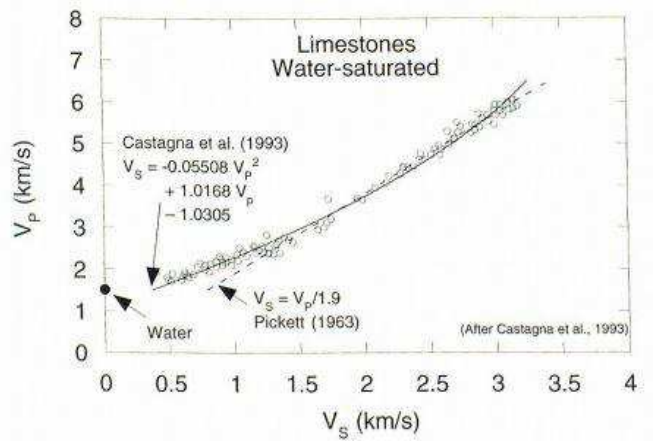

Figure 7: Castagna et al. (1993) and Pickett's (1963) correlations for limestones.(Mavko et al., 1998)

Dolomite

Similarly, the correlations for water-saturated dolomites were made by Castagna et al. (1993) and Pickett (1963). First, the Pickett's correlation (Mavko et al., 1998):

$$V_S = V_P/1.8 \tag{37}$$

Second, Castagna et al. (1993) fit:

$$V_S = -0.583V_P - 0.078 \tag{38}$$

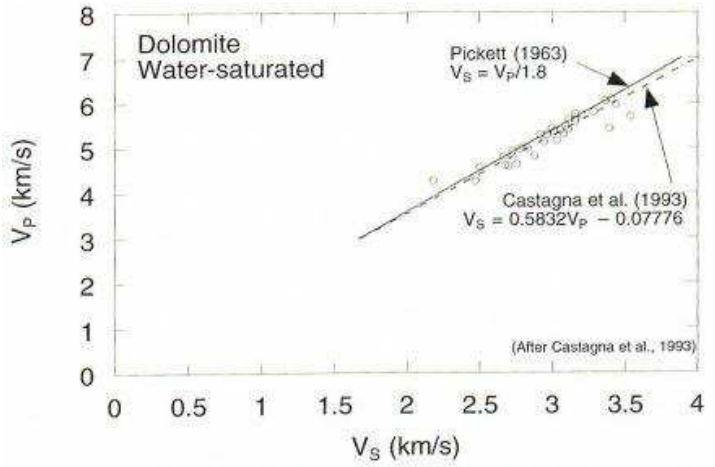

Figure 8: Castagna et al. (1993) and Pickett's (1963) correlations for dolomites.(Mavko et al., 1998)

Sandstones and shales

The best fit showed the correlation from Castagna et al. (1985), which was derived from in situ data:

$$V_S = 0.862V_P - 1.172 \tag{39}$$

and from Han (1986), which is based on laboratory ultrasonic data:

$$V_S = 0.794V_P - 0.787 \tag{40}$$

The correlations are very similar and give the best overall fit to the sandstones. Castagna et al. (1993) suggest that if the lithology is known, one can tune these relations to slightly lower V_S/V_P for high shale content and higher V_S/V_P in cleaner sands (Mavko et al., 1998).

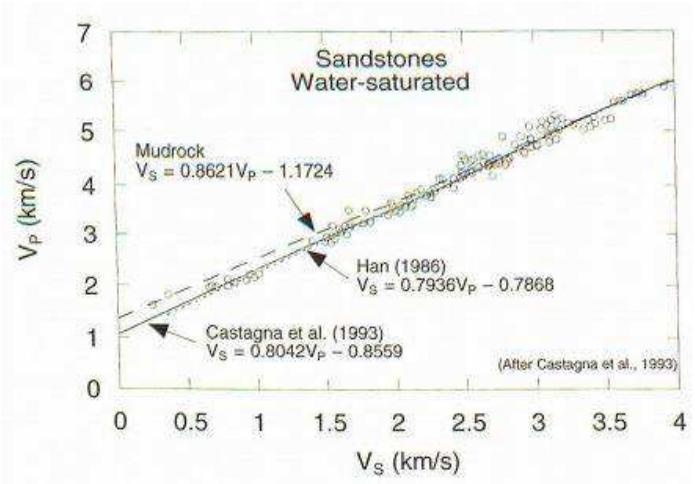

Figure 9: Castagna et al. (1993) and Han's (1986) correlations for sandstones. (Mavko et al., 1998)

Furthermore, studies were done where Han (1986) separated sandstones into porosity greater than 15 percent and less than 15 percent. The relations are as follows (Mavko et al., 1998):

$$V_S = 0.756V_P - 0.662 \qquad \text{porosity} > 15\% \tag{41}$$

$$V_S = 0.853V_P - 1.137 \qquad \text{porosity} < 15\% \tag{42}$$

2.4 VELOCITY – DENSITY RELATIONS

There are many applications where only V_P is known, and density or V_S must be estimated empirically from V_P. Here, the most useful correlations will be shown. Castagna et al. (1993) presented a very good summary of the correlations. Cracks and grain boundaries decrease the velocities. Therefore, the relations are expected to be more reliable under high effective pressures and fluid saturation. In the table below, Castagna et al. (1993) presented some velocity-density relations (Mavko et al., 1998).

Table 4: Polynomial relations of velocity-density dependance as presented by Castagna et al. (1993). Units are km/s and g/cc for velocity and density, respectively. (Mavko et al., 1998)

Coefficients for the equation $\rho_b = \boldsymbol{a}V_P^2 + \boldsymbol{b}V_P + \boldsymbol{c}$				
Lithology	**a**	**b**	**c**	**V_P range (km/s)**
Shale	-0.0261	0.373	1.458	1.5 – 5.0
Sandstone	-0.0115	0.261	1.515	1.5 – 6.0
Dolomite	-0.0235	0.390	1.242	4.5 - 7.1
Limestone	-0.0296	0.461	0.963	3.5 – 6.4

2.5 LINEAR CORRELATIONS

Empirical correlations and their usage are shown in the thesis. Because these are all correlations between two variables, it is worth describing one of the ways to correlate them. Unfortunately, due to costly UCS test this method was not used as experimental part of the thesis. However, the method is suggested as recommended in the discussion chapter.

As the name suggests, if two variables vary together and a relationship exists between them, then relationship can be assumed as linear. If the relationship is positively linear, then they both increase or decrease together. If the relationship is negatively linear, then one rises and the other one drops. To connect two variables we basically need to fit a straight line to the results we obtain.

Results of any measurement follow certain pattern, which can be approximated with unknown function. Linear relationship is the simplest form of correlation. Random results, grouped around a line are seen in the figure below. It is impossible to define these measurements in functional sense, since the points are not on the same line. It is possible to draw infinite number of lines through these points. But only two can adjust to all points (Mihailović, 2002):

$$Y = a \cdot X + b \tag{43}$$

And

$$X = A \cdot Y + B \tag{44}$$

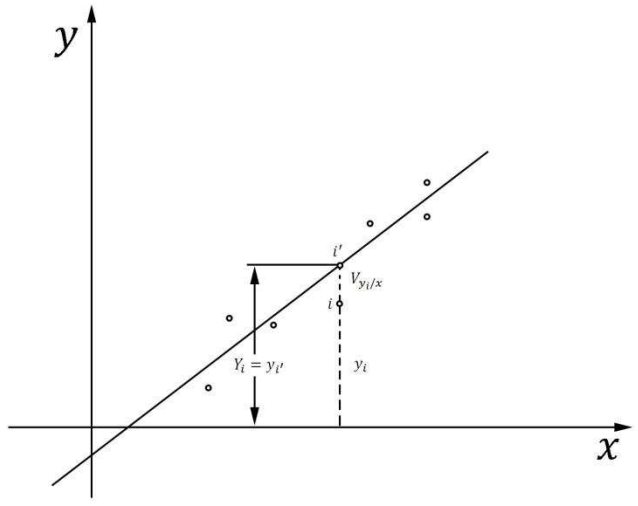

Figure 10: Random results with a line which fits the best. (Modified after Mihailović, 2002)

Parameters a and b can be defined when sum of the least squares of $V_{y_i/x}$ is minimum:

$[VV]_y = min.$,
and A and B, with sum of the least squares of $V_{x_i/y}$ is minimum:
$[VV]_x = min.$

If $Y_i = y_i + V_{y_i/x}$ is inserted into the equation 43, then it yields:
$y_i + V_{y_i/x} = a \cdot x_i + b, i = 1,2, \dots, n$

Because $x_i = const.$, only corrections for y_i are made with $V_{y_i/x}$. The system has more known values than unknowns. Therefore, parameters a and b can be defined with the least squares method. Parametric equations are as follows:

$$V_{y_i/x} = a \cdot x_i + b - y_i \tag{45}$$

hence:

$$V_{y_i/x} = a \cdot \left(x_i - \frac{[x]}{n}\right) - \left(y_i - \frac{[y]}{n}\right) = (x_i - \bar{x}) \cdot a - (y_i - \bar{y}) \tag{46}$$

where $\bar{x}$ and $\bar{y}$ represent mean values:
$\bar{x} = \frac{[x]}{n}, \bar{y} = \frac{[y]}{n}$
It follows that:

$$a \cdot [(x_i - \bar{x})^2] - \big((x_i - \bar{x}) \cdot (y_i - \bar{y})\big) = 0 \tag{47}$$

and

$$a = \frac{(x_i - \bar{x}) \cdot (y_i - \bar{y})}{(x_i - \bar{x})^2} = \frac{K_{x,y}}{S_x^2} = r_{x,y} \cdot \frac{S_y}{S_x} \tag{48}$$

because

$$K_{x,y} = \frac{[(x_i - \bar{x}) \cdot (y_i - \bar{y})]}{n - 1} = r_{x,y} \cdot S_x \cdot S_y \tag{49}$$

$$S_x^2 = \frac{[(x_i - \bar{x})^2]}{n - 1} \tag{50}$$

$$S_y^2 = \frac{[(y_i - \bar{y})^2]}{n - 1} \tag{51}$$

When the equations 45 are divided by n, then it yields:

$$\bar{y} = a \cdot \bar{x} + b \tag{52}$$

and if the equation is rearranged:

$$b = \bar{y} - a \cdot \bar{x} \tag{53}$$

Because $\left[V_{y_i/x}\right] = 0$, which follows from $V_{y_i/x} = a(x_i - \bar{x}) + (y_i - \bar{y})$.

Parameter a can be derived from equation 48 and parameter b from equation 53. With these parameters known, approximation of the real values $M[a] = \mu_a$ and $M[b] = \mu_b$. Approximation of the regression line is calculated by the following equation:

$$Y - \bar{y} = r_{x,y} \cdot \frac{S_y}{S_x} \cdot (X - \bar{x}) \tag{54}$$

In regression analysis measured results are approximated with the line which fits these results the best. As such, two possible cases exist. The first case, which is described above, estimates that for already known values x_i $(i = 1,2, \dots, n)$ measures the corresponding values of y_i $(i = 1,2, \dots, n)$, which are normally distributed $Y \in N\left(\mu_y, {\sigma_y}^2\right)$. The second case appears when both values x and y and the results x_i $(i = 1,2, \dots, n)$ and y_i $(i = 1,2, \dots, n)$ follow normal distribution $X \in N(\mu_x, {\sigma_x}^2)$ and $Y \in N\left(\mu_y, {\sigma_y}^2\right)$. (Mihailović, 2002)

In the case of this thesis, the first case is sufficient. Ideally, we would have two sets of data; one set about rock strengths (from the same rock, formation) and the second set would be measured porosity or sonic velocities. X would represent the rock strength and y porosity or second velocity, respectively. Obviously, higher number of measurements is preferred.

To make calculations easier an Add-in such as “matrix.xla” can be used in MS Excel. It has function “MCorr”, which makes the correlation in a matter of few clicks. It uses the matrix principle and should therefore be used as matrix calculation.

3 BHA DESIGN AND DRILLING DYNAMICS

3.1 BHA DESIGN

BHA design is one of the most important elements while drilling a directional well. It affects drillability, wellbore stability, hole quality and drilling direction. The BHA is the portion of the drillsting that affects the trajectory of the bit and, consequently, of the wellbore. Its construction could be simple, having only a drill bit, collars, and drillpipe, or it may be complicated, having a drill bit, stabilizers, magnetic collar, telemetry unit, shock sub, collars, reamers, jars, crossover subs, heavyweight drillpipe, and regular drillpipe. The BHA design is dependent on many factors including, but not limited to (Buorgyne et al., 1986):

- Bit side force.
- Bit tilt.
- Torque while drilling.
- Components wear.
- Riguosity of the hole (hole enlargement).
- Hydraulics.
- Formation dip.
- Formation rock properties, especially (but not only):
    - Uniaxial compression strength.
    - Friction factor.

In the thesis more attention will be given to the latter two factors – effect of formation dip and formation rock properties. Because BHA is within the formation, it is clear that BHA itself affects the formation and that the formation reacts back on the BHA. This reaction of one on the other will try to be analysed in details. This greatly influences the direction of the wellbore, wear of BHA and wellbore stability including stuck pipe problems.

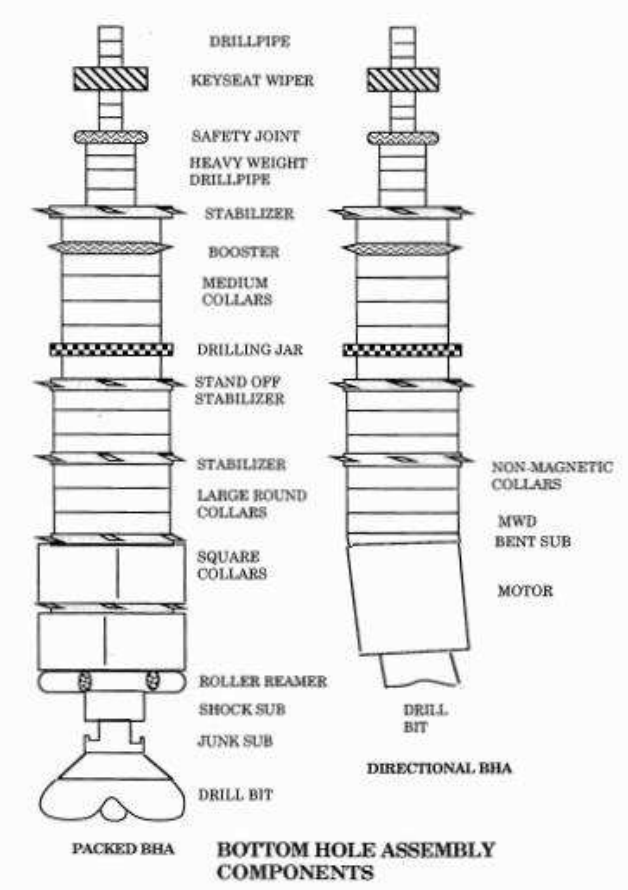

Figure 11: Typical scheme of packed and directional BHA. (Buorgyne et al., 1986)

Many other parameters are indirectly or directly affected by the formation properties, for instance bit tilt. The tendency of the bit to build, to hold, or to drop angle is based on a positive, zero, or negative side force. Essentially, this would be the case for hard formations where drilling rates are below 10 ft/hr. When the formation is soft to medium-hard, the side-fore tendency is not the only component that will influence the inclination and direction of the bit. Because of the curvature of the BHA near the bit, the bit is canted or tilted in some resultant direction and inclination, somewhat like the bent housing and bent sub. In such case, the magnitude of the tilt is directly influenced by the strength of the formation. Just as a deflection tool will not obtain the maximum curvature for which it was designed in harder formations, so it is with a BHA a given bit tilt. For instance, in very soft formations, where drilling rates exceeding 100 ft/hr, the side force again can be the predominant mechanism and will, in many cases, mitigate the effects of BHA bit tilt. When the formations are soft to medium or where drilling rates are between 10 and 100 ft/hr, effects of the bit tilt can be significant. (Buorgyne et al., 1986)

The packed BHA and direction BHA are presented, as seen in the figure above. Packed BHA are quite popular but they do not drill more vertical holes and they can't drill directional holes. However, they have many advantages over other BHA types. For example, they protect the drillpipe in the drillsting, reduce rough drilling, reduce severities of doglegs, increase drill

bit performance and drill straighter holes. Therefore, they are often used for drilling hold sections. Whenever, there is a need to drill a directional well, directional BHA should be used. The main functions of such BHA are to build the inclination, drop the inclination, walk right or left and drill straight ahead, if needed. However, RSS motors and other techniques are used nowadays which changes the BHA design significantly compared to ones in the past.

The formation strength and formation dip have the greatest effect on directional control of the BHA. That is the reason why, ideally, drilling should be conducted perpendicular on the dip. If drilling occurs in angle of attack less than 90°, then the bit will go in direction of the dip.

For optimal BHA design proper software should be used. Chen (2007) proposed software with equilibrium dogleg severity rate prediction, force analysis, formation index calculation, predict ahead analysis, sensitivity analysis, survey sag correction calculation and whirl detection. The features use static and dynamic models. He claims that this is the most accurate program in the industry. Furthermore, he verified it and compared it with other softwares in the field which has confirmed his statement.

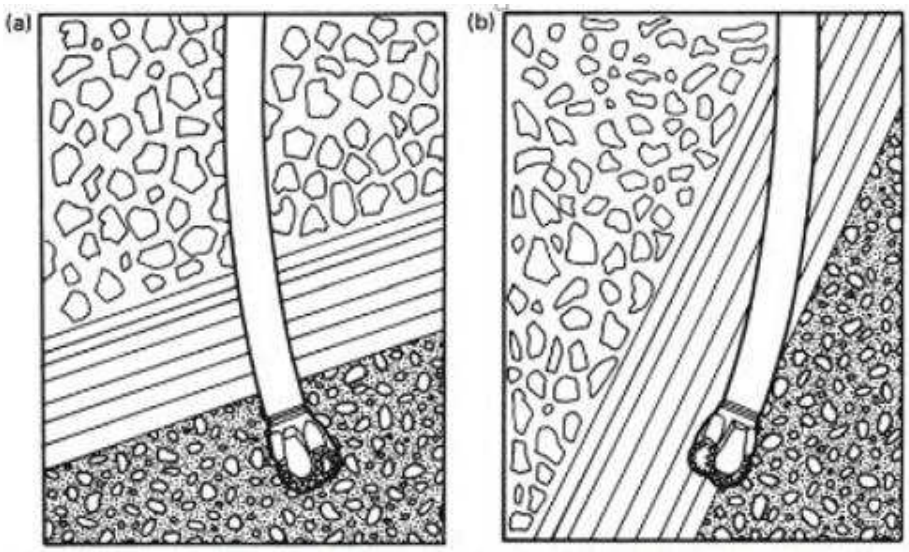

Figure 12: Effect of a formation dip can be observed. Additionally, perpendicular (a) and parallel (b) angle of drilling are shown. If the angle is not perpendicular then the direction of drilling will be in the direction of a dip. (Inglis, 1987)

BHA design must meet many specific criteria. Directional requirements, tool requirements, hydraulics requirements, component availability, drilling optimization or operational requirements may all have higher priority than vibration control in BHA design, but they are all connected. (Chatar et al., 2011)

BHA design has a direct impact on how the drillstring responds to interaction between its components and formation. Moreover, rock properties such as friction and rock's strength affect both, BHA design and the BHA oscillation response. The next chapter will focus on drilling dynamics in general and how geomechanical properties affect it.

3.2 DRILLING DYNAMICS

Drilling dynamics principles will be discussed in this chapter. The thesis focus is how different geomechanical properties influence drilling dynamics. Before general drilling dynamics is explained, the most important parameters should be mentioned. The uniaxial compression strength, which is part of the experiment in the chapter 4, is the first important property. Friction factor of tools and the wellbore is the second factor, which directly influences vibrations. These two properties are discussed in more detail in the chapter 3.2.1. The geomechanical knowledge about formation drilled is crucial in order to avoid or mitigate all the severe dysfunctions which are discussed in the next paragraphs.

During drilling operations many movements occur and there are many parameters which influence them. For any drilling operation, certain weight on bit is applied, the drillstring rotates (except if PDM is used), the mud must be pumped, the formation acts on the drillstring, and the drill bit is in direct contact with the formation. All these interactions affect the bit, BHA and drillstring. The processes that are going on between these elements are termed as drilling dynamics. As the name suggests, these are all dynamic and not static models. Elimination of reduction of severe drilling dynamics performance may require advanced planning and BHA design, changing operating parameters or use of a new technology. All of these are focus of this chapter. In this chapter principles of drilling dynamics will be researched, with a special emphasis on how different rocks affect it. Some case studies will be shown and as a result the best practices will be given.

Firstly, the source which starts dynamic behaviour should be addressed. The most observed one is between a rock and the bit. When the bit is on bottom it reacts with a rock in some way. The energy which is produced between these two elements can be transferred further to the BHA. Additionally, there are also other sources which can start excitation of the BHA, for instance the mud pumps and the stabilizers. A stabilizer with four straight blades was found to generate a signal at a frequency of four times RPM. For comparison, the excitation frequency of the rock and bit interaction is of three times RPM (Burgess et al., 1987).

Secondly, some phenomena should be described. One of them is so called stick/slip behaviour. It appears when nonlinear wellbore friction induces a torsional pendulum motion in the BHA. The frequency of this oscillation is usually lower than the fundamental torsional

frequency of the BHA and it may never be noticed if there is no dynamic data. Its impact is significant and it is an important feature of the drillstring dynamic behaviour. One way to minimize this destructive phenomenon is to adjust surface RPM when one receives a torque feedback (Payne, 1992). Another explanation is that this is a torsional oscillation of the BHA while rotary drilling, where BHA stops rotating for part of its torsional cycle and then breaks loose and rotates at high angular velocity until it stops again (Nicholson, 1994). In a situation where stick/slip behaviour is excited because of high frequency oscillation, it can absolutely stop the BHA (to zero RPM) and then accelerate up to 300 RPM. Such behaviour can lead to failures (Oueslati et al., 2014).

Lateral and axial vibrations are another type of movements of the BHA. They can be caused because of a cycle of tension and compression of the BHA components. Consequently, the movements can induce vibration harmonics. The amplitude and frequency of these harmonics increases with time and it produces a chaotic motion. They can often occur as shocks. (Ramizer et al., 2010)

Another motion or phenomenon is known as the BHA whirl. It can occur when the BHA is affected by torsional vibrations which are started because of the high rotational friction caused by formation, for instance. Such motion can also be termed as a backward whirl. It can be observed on the surface by the counter clockwise movement of the drillpipe around the rathole and stalling of top drive (Ramizer et al., 2010). We distinguish between a few whirls. First, pure forward synchronous whirl can occur, which means that drill collars whirls in the same direction as it is rotated, and the whirl and rotary frequencies are the same. Second, nonsynchronous forward whirl can occur, which means that the directions are the same but the frequencies are not equal. Additionally, backward and chaotic whirl exist where chaotic whirl means that there is neither predictable motion nor frequency. However, all whirls involve stress cycling and therefore accelerated fatigue rates (Mason et al., 1998). Usually, BHA whirl cannot be seen on the surface. The only indication might be a slight increase in surface torque. Therefore, downhole tools should be used to detect increased bending moment and lateral acceleration (JPT, 1999).

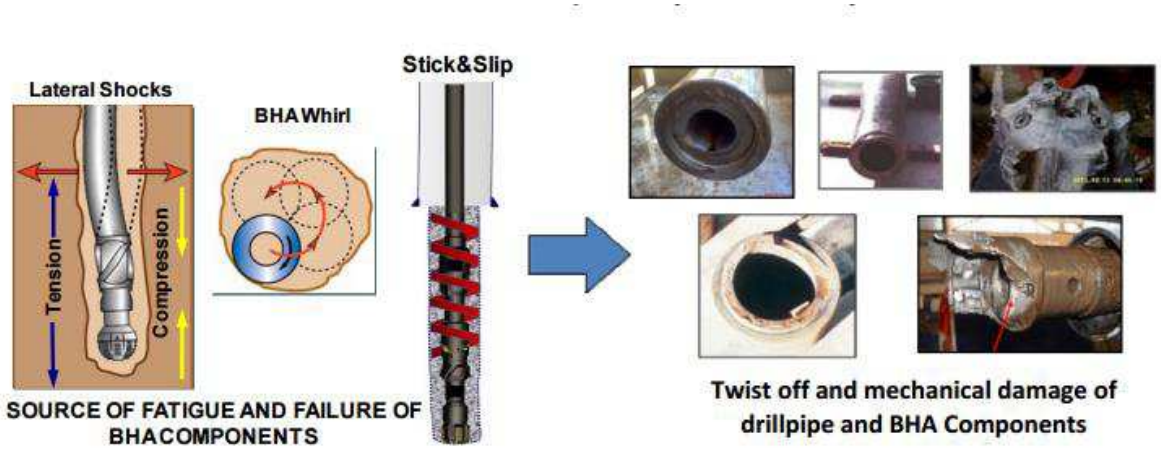

Figure 13: Some of the vibrations in the BHA and their possible consequences. (Ramizer et al., 2010)

Nicholson (1994) described a few natural modes of lateral vibration. When the BHA is rotated at an angular velocity equal to a natural frequency of lateral vibration, it will bow out in its natural mode shape while performing forward synchronous whirl. If the borehole is in gauge and therefore lateral support is provided to the bit and stabilizers, then the drillstring can be analysed for its natural frequencies of lateral vibration and associated mode shapes. Effects of drillstring tension, drilling fluid buoyancy and added mass need to be included in the model. The resulting natural frequencies are lateral vibration critical rotary speeds. Lateral vibration critical rotary speeds are those at which the drillstring may initially perform forward synchronous whirl which may then result in dynamic contact of the drill collar with the borehole wall resulting in lateral shocks or backward whirl.

All these phenomena need certain excitation frequency or energy. The frequency is often overlapping with the drilling operating frequencies, such as pump stroke, rotary speed, motor speed, turbine, etc. The relationships can be seen in Figure 14.

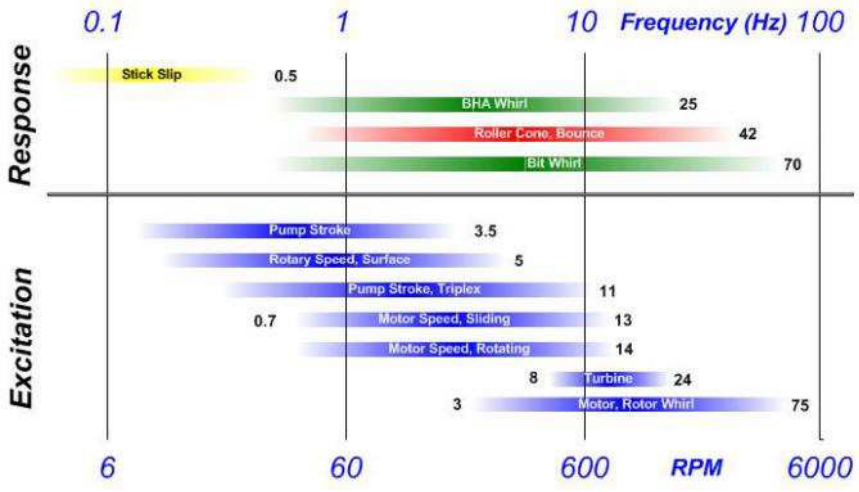

Figure 14: Relationships of some known excitation frequencies to the frequencies of dynamic behaviour.(Reckmann et al., 2010)

With changing only operational parameters, vibration effects may improve, but the drilling performance can significantly decrease. If there is no extra information regarding expected drilling dynamic behaviour, identification of the root cause of the problems may be impossible. Therefore, the drilling dynamics problems should be addressed as a symptom of a problem that needs to be corrected through appropriate action which, in addition to changes in operating parameters, may include changing the drillstring and/or BHA design, changing the bit type, installing a torque feedback control system, etc. (Nicholson, 1994)

All the effects described until now occur with low frequencies. With better technology and methods, high frequency rotations were recorded in the field. BHA torsional vibrations and tangential acceleration can be especially harmful. These vibrations occur at much higher frequencies than drill collar resonance and are significantly depended on the drilled formation. The vibrations occurred at much higher frequencies at more than 240 Hz which is more than what was believed before. Interestingly, high frequency torsional oscillations occur at higher WOB and low-to-moderate revolutions. This was found in a laboratory and was also confirmed in the field. These vibrations are excited by the drilling bit and are usually not harmful to the bit itself. However, they can excite a natural frequency of the BHA or the whole drillstring, which can result in tool failures and NPT. (Oueslati et al., 2013 and Jain et al., 2014).

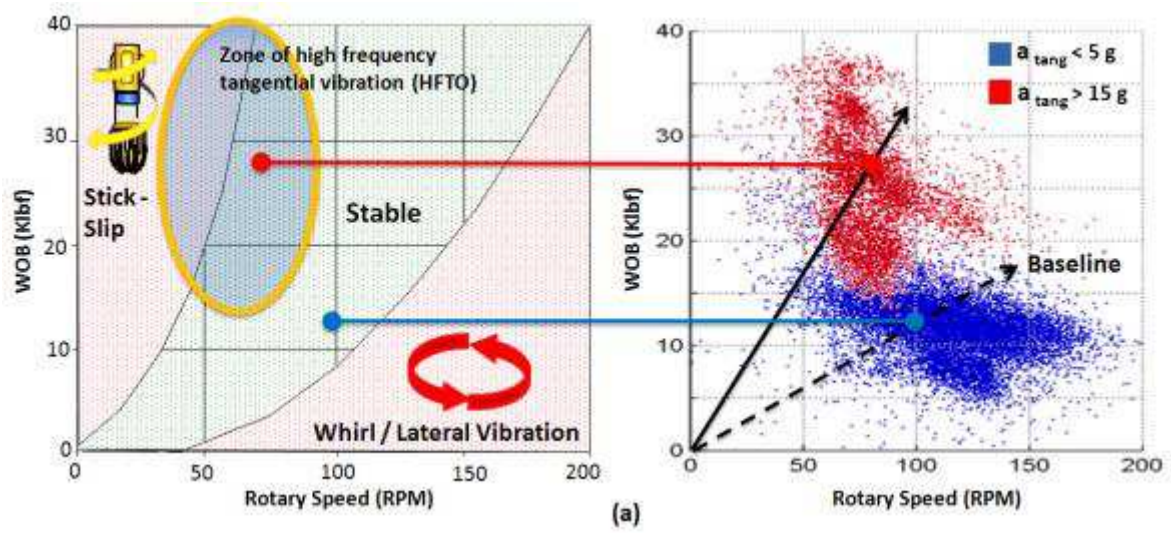

Figure 15: WOB versus rotary speed relation and drilling dynamics dysfunctions which can occur. (Jain et al. 2014)

3.2.1 Formation effects on drilling dynamics

BHA interacts with the wellbore wall and vice versa. In the previous paragraphs, general dynamic behaviours were described and their possible consequences were mentioned. Drilling

dynamics is already a complex topic within itself, but it gets even more complex when formation effects are taken into account. How the BHA is influenced with formation depends on the BHA design, drilling parameters, borehole clearance and the formation itself.

Drillstring or BHA dynamic behaviour can be correlated to the formation being drilled. Thus, the bit is established as a critical excitation source. High frequency measurements, both surface and downhole, disclose complex effects including drillstring/casing interaction, transient boundary conditions, a multitude of excitation mechanisms, and unpredictable walking and whirling patterns. These observations suggest that many dynamic phenomena extend beyond available drillstring modelling technology. Certain problem complexities should probably be avoided to allow focusing on the most critical aspects. Approximately three decades ago, exact modelling of the BHA and wellbore contact was not feasible due to lack of powerful computational technology. (Payne, 1992)

One of the most observed interactions is when the BHA enters in lateral resonant motion, due to drilling vibrations, it hits the formation (BHA shock) with a certain force that increases the level of vibration in the entire drillstring. If another shock is induced in sync with the vibration harmonics, the BHA enters in a frequency of multiple shocks of high magnitude. Drilling with constant and especially high or extreme level of shocks provides the environment for a potential of failure in downhole electronics of LWD, MWD, RSS which results in non-productive time and extra costs (Ramizer et al., 2010).

Interestingly, the most severe vibrations occur when drilling from soft formation to a hard abrasive formation. A question arises, what is happening with the BHA in the soft formation while the bit is drilling the hard one. There are many case studies in which they analysed and were trying to optimize BHA design and minimize non-productive time (see the case studies).

Oueslati et al. (2013) observed a correlation between tangential vibration and formation properties. They plotted tangential acceleration over the depth and superimposed to formation properties, such as bulk density and gamma ray count. There is a correlation between the occurrences of tangential vibration and formations with low gamma ray count and high bulk density. Additionally, statistical analysis was done and proved that tangential vibration associated with HFTO (high frequency torsional occurrence) occurs mostly when drilling hard formation with low gamma ray count and high bulk density. The same correlation was confirmed by study of Jain et al. (2014). Interestingly, the gamma ray parameter seems to be the primary factor influencing tangential vibration. A possible application is the use of the measurements in general and tangential acceleration in particular as an early indicator for formation change. If dynamic measurements can be placed closer to the bit and several meters

below LWD tools, then they can detect the formation changes earlier and help the crew to prepare and make decisions to mitigate vibrations and improve performance.

Stick slip occurrence was correlated to bulk density in a carbonate reservoir in Saudia Arabia. Stick slip index increased when bulk density of the formation increased. Additionally, a relationship between low gamma ray and high tangential accelerations was found. These relationships were found for several wells within the same reservoir. Bulk density and gamma ray data could greatly help with drilling dynamics prediction and its real time monitoring (Al-Shuker et al., 2011).

As mentioned before, many failures occur while drilling through a relatively soft formation which includes some harder stringers. In a study of Hood et al. (2003) major issues were found while drilling relatively loose sand with hard calcite cemented zones. The issues included high doglegs which accelerated fatigue of the BHA components and connections. During drilling a bending measurement device was used. When the hard calcite stringers were drilled, a significant increase in bending moment and inclination angle was found. A lot of time was lost and many tools failed. It is interesting that that when the bit hit the calcite stringer at a low dip angle, it followed the path of least resistance into the loose sand. Because one part of BHA was in the loose sand and another part in the calcite, the bending moments increased over all limits and the target depth was not reached. Additionally, the bit and some sensors failed. In conclusion, this example confirms that drilling dynamics dysfunctions are directly related to rock properties.

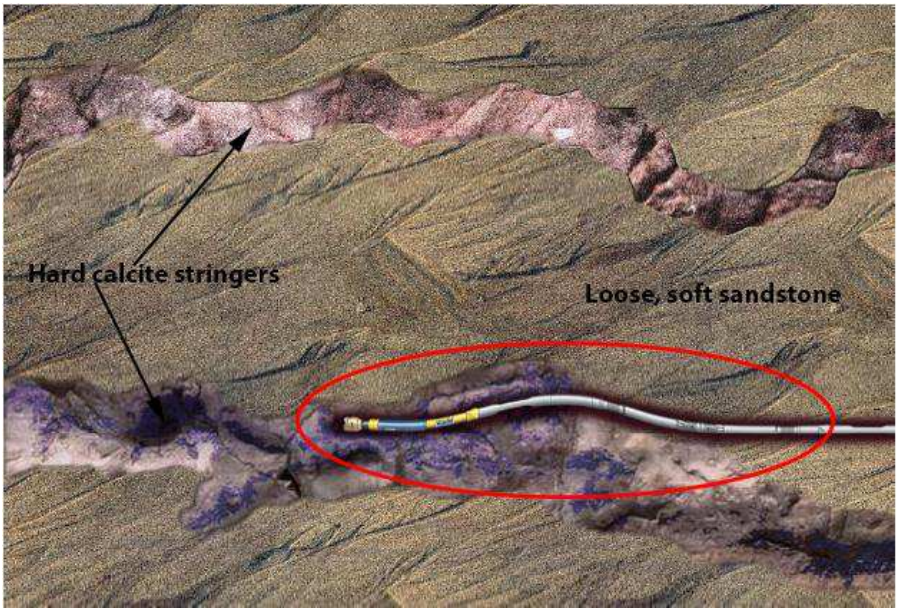

Figure 16: The figure is representing drilling through loose, soft sandstone with hard calcite stringers. The question arises what is happening with the BHA in such conditions. (Modified after Hood et al, 2003)

A borehole size is another important parameter which directly influences drilling dynamics. The larger holes allow vibration energy to build up in the BHA without making wall contact which would dampen harmonic vibrations. Usually, lateral vibrations significantly increase in wellbores bigger than 12-1/5 inch which means that the borehole size matters especially in the upper sections, whereas in deeper sections boreholes are usually smaller. (Allen, 1987)

Friction factor

Friction factor of a rock is another important parameter which affects drilling dynamics. It is especially important in long reach wells with a long horizontal part. One of the analyses, where friction factor has a great importance is torque and drag analysis. Drag is excess load compared to rotating drillstring weight, which may be either positive when pulling the drillstring or negative while sliding into the well. This force is generated by drillstring contact with the wellbore wall. When rotating, this same friction will reduce the surface torque transmitted to the bit. Therefore, it is useful to be able to estimate the friction forces when planning a well (Mitchell et al., 2009). Additionally, friction between a tool and a wellbore can cause sinusoidal or helical buckling. Furthermore, buckling can cause stress cycling, which increases fatigue of a material and can result in failure (Mirhaj et al., 2010, Gee et al., 2015). However, it should be noted that friction factor in a wellbore does not solely depend on formation itself, but also on: (1) cutting bed thickness, (2) cutting composition and characteristics and (3) filter cake (Quigley et al., 1990).

Buckling and different friction factors at different points in a wellbore can also excite severe vibration phenomena, such as stick slip (Gee et al., 2015). Figure 16 represents how different rock strengths affect BHA. If we drill through different rock types, they certainly have different friction factors, which will result in different responses along the BHA. Therefore, it can be concluded that different rock strengths also mean different friction factors (since this means different lithology). To sum it up, friction factor greatly influences drilling dynamics and can cause dysfunctions like stick slip, BHA whirl and high tangential oscillation.

3.2.2 Issues with the measurements of drilling dynamics

In order to make an analysis, data must be collected. Ideally, the data should be as close to the source of interest as possible. Often, this is not the case, because the BHA design. However, tools got more advanced and they make it possible to measure all vibrations at all frequencies.

A problem appears that many operations are not monitored because of using improper tools. The reason of this is that only axial vibrations, torsional vibrations and lateral vibrations are possible to measure with standard vibration sensors. Whirl, tangential accelerations and bit

bounce can be measured with advance dynamics tools only (Al-Shuker et al., 2011). Consequently, the special tools are expensive and therefore not so commonly used. One of the issues is also limited bandwidth and range of sensors in downhole devices. To correctly measure a signal, the theoretical minimum sampling rate must be at least twice the highest frequency component of the signal. Realistically, the sampling rate must be more than just two times higher than the highest frequency to enable for the necessary filtering that removes unwanted signal components (Jain et al., 2014). To sum it up, there are at least three limitations conducting such measurements: (1) the cost can be prohibitive which can preclude the use of a tool even when dynamic dysfunctions are suspected, (2) the tool may be on a distance of 10 – 100 feet from the bit and the data may not represent the conditions at the bit and (3) the sub-based tools alter the BHA (Pastusek et al., 2007)

It is often hard to place sub-based sensory below a motor because this adds length to the BHA and additional bending load to the bearing housing (Pastusek et al., 2007). However, to overcome such issues new tools were developed. Such a tool can be seen in the figure below. A benefit of this tool is that the distance to bit is very short. Other accelerometers can be then placed in the BHA, behind the MWD and LWD unit. In this arrangement one can have a very good understanding of the dynamics.

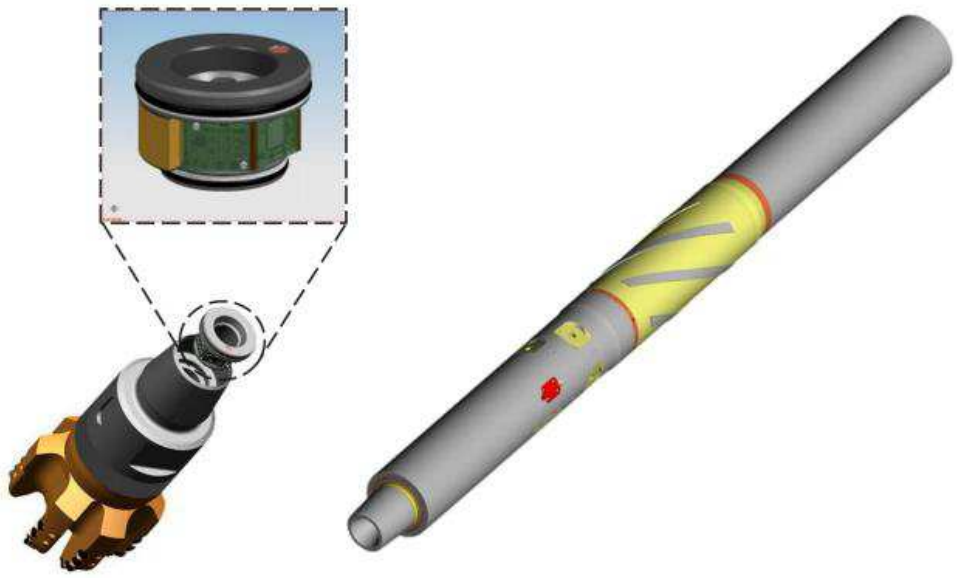

Figure 17: Modular vibration sensor, positioned just after the bit. (left) and a typical MWD tool (right). (Oueslati et al., 2014)

In the next chapters a few relevant case studies are summarized. Because it is rather hard to put all real examples into one homogenous text, I decided to include the most relevant case studies that show drilling dynamics issues in a very clear manner. First, the problems are identified in the studies. Second, properties of the wellbore, geology, location and other

parameters are described. Additionally, formation and borehole effects are analysed. Last, the used solutions and improvements are given. As a result, recommended practices and recommendations can be given.

3.2.3 Case study 1 – Ramizer et al., 2010

This study was done on young fields in Mexico. The biggest problems occurred in 17 ½" borehole section with high lateral and torsional BHA vibration, which resulted in costly drilling incidents, like, drillstring twist off, physical damages, and failures of downhole tools. Interestingly, the average non-productive time per section per well was 15 days.

The problem of vibrations is focused mostly between the depths of 1000 m and 1500 m. The interesting profile to look at it is the lithology of the section drilled. Interestingly, the highest vibrations occurred when drilling from soft shale to abrasive and high strength sandstone. This transition caused BHA to fail, fishing, side tracking and NPT up to 19 days. Tool failures can be seen in Figure 13.

Different types of vibration in this section (shale-sand) initiate when the bit moves from drilling soft shale at high penetration to hard, abrasive sand at high UCS; the bit will slow down and the drillstring enters higher compression as the driller applies higher weight on bit to maintain the same ROP that was seen in the shale layer. This causes a cycle of tension and compression of drillstring components and induces vibration harmonics along it as well. The amplitude and frequency of these harmonics increases with time and it produces a chaotic motion when the BHA enters in torsional vibration due to the high rotational friction caused by the abrasive sands. This motion is referred to as backward whirl. This type of vibration is reflected on the surface by the counterclockwise movement of the drillpipe around the rathole and stalling of top drive. Stick and slip and BHA whirl are two types of vibration that has devastated the integrity of the drillpipe and BHA components used in these wells.

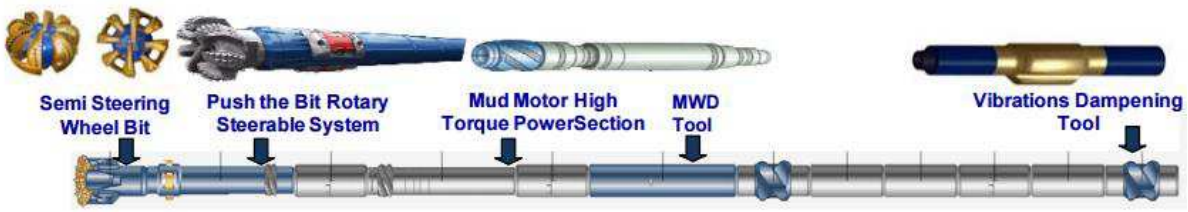

Figure 18: Redesigned BHA which improved drilling time for 300%.

The solution which was used to solve the problems was rather simple. The BHA design was redesigned, and for problematic section mud motor plus insert bit were used. For the uniform section where there was no change in lithology, RSS with PDC bit was used. With this design

the results were much better but such design still requires on trip. It is in interest of any operator to have the lowest number of trips. To achieve this, they combined advantages of both BHA designs. As a result, powered RSS was used, as seen in Figure 18. The bit featured ring at the gauge diameter which helps reducing lateral forces at the lower BHA. The design reduced vibrations and kept them to a minimum. The only problems was at the upper BHA, where lateral accelerations were a bit higher. Because of that, vibration dampener was added at the upper BHA and as a result, the lateral accelerations decreased for 50 %. Overally, results were very good, with a 100% improvement of ROP and the TD was reached 28 days faster than in previous cases.

3.2.4 Case study 2 – Mason et al. (1998)

Mason et al. (1998) addressed BHA whirl in the Mobile Bay. Different rock strengths, from soft chalk to abrasive and strong limestone. Because there was no monitoring prior this experiment, many BHAs failed due to high magnitude and fatigue. Another reason was washout hole – larger clearance, better conditions for whirl. Therefore, combination of both helped BHA to fail.

When real time monitoring was implemented, it showed that drillstring vibrations were affected by high-amplitude rotary peaks. It was found that the anomalous peaks occurred because of BHA whirl which could be confirmed with no significant wear of the bits. Another interesting problem was found: a washout which increased BHA whirl occurred, therefore was not clear if the washout occurred because of the whirl and if the washed hole cause greater fatigue rates during whirl. They concluded that the primary cause of the drillstring failures in the Mobile Bay wells is BHA whirl in washed out hole. When the proper anti-whirl measures were taken the incidence of failure was greatly reduced and the performance was greatly improved.

3.2.5 Case study 3 – Bailey et al. (2009)

In this study, redesign of a 12 ¼ inch motor BHA was done. Prior the study, roller reamers were introduced to the BHA and they caused significant reduction in the need for back reaming. However, the problem was that cracking of the roller reamer body was observed in several runs. To solve this problem, they moved the roller reamer within the BHA to a position above one or two joints of HWDP.

After the redesign, the problem of cracking disappeared and an increase of 36 % in ROP was achieved. In other words, the probability of cracking the roller reamer was reduced from 50 % to 0 % because of the design change.

Mechanical specific energy analysis, confirmed a significant improvement of the new design. According to the authors experience, a tool failure usually occurs if the MSE readings often exceed 100 ksi. The new BHA had MSE readings well below 80 ksi which decreased a tool failure probability.

With a proper designed BHA, drilling vibrations can be significantly reduced which results in increased footage per day and reduced tool damage. It has been found that a proper redesign has lower calculated vibration indices than the standard BHA. Performances increased up to 36 %. Additionally, the probability of cracking the tools (roller reamer) was reduced from 50% to 0% and bit wear was smaller with longer runs than with standard BHA. (Bailey et al., 2009)

Additionally, drilling dynamics analysis was done for drilling a vertical 6 1/8 inch in a hard formation of interbedded sands and shales. Because a new bit was used, WOB was increased in order to maximize ROP. With increased WOB several directional problems occured. The problem was that the BHA was not laterally stable. The BHA was changed to a stiffer one but this resulted in much more severe dynamic response. Furthermore, such BHA design was more prone for tool failures because the shock risk and stick-slip indices were very high. It was also found that shock risk lowered at a certain depth because of the formation.

3.2.6 Case study 4 – Reckmann et al. (2010)

This case study was primarily done to mitigate and monitor MWD tool failures due to drilling dynamics behaviours. Real time monitoring and a huge database were included in the study. The data were recorded at five seconds interval and the data were collected from more than 12,000 drilling hours or, more than 425,000 feet drilled.

The MWD tool, which was used during drilling, is capable of taking 14 dynamic measurements at a sample rate of 1,000 Hz, among them lateral, axial and tangential accelerations, torque, axial force, and bending moment. These data are available in real time. Additionally, the data are stored in the downhole memory with a sampling interval of five seconds. In total, 232 data sets were gathered and 67 of these contained identified vibration related failures.

Several parameters such as cumulative rotary speed variance, relative energy, backward and forward whirl and stick-slip index were taken into account. With a help of binary logistic regression, they determined which parameters are significant and which one are not

significant. This test showed that cumulative energy, due its lateral motion of MWD, is the most significant.

A table was presented which shows how fast the tool fails under certain lateral motion, as seen in Figure 19. It is observed, that if the tool is stressed with more than 3 g, then it will not last longer than approximately 60 hours with a 100% probability to fail. If the tool is below 3 g, then it can last up to 140 hours with the highest probability to fail at 0.6. These data can be used as a powerful method of tracking the condition of an MWD BHA or BHA. It relates current vibration level to likelihood of failure, and provides an estimate of remaining lifetime to failure.

The third most significant parameter contributing to failure was the cumulative rotary speed variance. When evaluating this parameter, one should consider that cumulative rotary speed variance differs for different tool sizes. The strongest relationship was found for 5.75" tool size.

Whirl was also found statistically significant in tool failures. The whirl is destructive because it can result in high cyclic bending stresses and also in high lateral accelerations. The short time spans of whirl to reach high probabilities of failure show the destructive effect of it on the BHA. Therefore, real time monitoring of it is necessary.

Another interesting analysis was done in the study. Rate of penetration versus lateral acceleration and stick slip index was plotted. Surprisingly, the highest ROP was found where low lateral vibration and non-zero stick-slip index (around 0.5) occur. However, an optimal operational region is around an SSI (stick-slip index) of 0.5 with the lateral vibrations less than 3 g which yields an average ROP greater than 50 ft/h.

P(f)	>0.5	>1	>1.5	>2	>2.5	>3	>3.5	>4	>4.5	>5	>5.5	>6	>6.5	>7	>7.5
1.0	∞	∞	∞	∞	126	60	27	15	9.5	6.5	4.5	3.1	2.1	1.3	0.7
0.9	∞	∞	∞	150	110	48	23	13	8.7	5.9	4.1	2.9	1.9	1.2	0.6
0.8	∞	∞	∞	143	88	38	19	12	7.8	5.4	3.7	2.6	1.7	1.0	0.5
0.7	∞	∞	∞	123	64	29	16	11	6.9	4.8	3.3	2.3	1.5	0.8	0.3
0.6	∞	∞	134	87	42	22	13	8.5	5.8	4.1	2.8	1.9	1.2	0.6	0.1
0.5	143	118	83	47	25	15	9.6	6.5	4.5	3.2	2.2	1.4	0.8	0.3	
0.4	70	50	32	19	12	8.4	5.8	4.1	2.8	1.9	1.2	0.6	0.2		
0.3	11	8.1	5.9	4.3	3.1	2.1	1.4	0.8	0.3						

Figure 19: Failure rate (probability) versus lateral 1s RMS accelaration threshold and time. (Reckmann et al., 2010)

3.2.7 Case study 5 – Elsborg et al. (2006)

Another interesting case study was done offshore Norway. The study includes drilling 24 inch deviated hole with the end inclination of 70° and length of 1300 m. The well was drilled using

a 17 ½" PDC bit, RSS system, and PDC hole opener. Because major issues and failures occurred during drilling, an extensive analysis was done using time and depth based data, formation information and vibration measurements from the offset wells.

While trying to drill the well, excessive vibrations caused tool failure, loss of hole angle and the section had to be ended earlier. For the next section, a 17 ½" pilot hole was drilled following a pickup of 24 inch PDC hole-opener. Afterwards, sever vibrations and non-optimal jar placement ended with the string twisting off followed by a fishing trip and three more unsuccessful hole opening attempts. Clearly, this was time consuming and costly operation.

The static calculations showed that there was no critical side fore, bending moment or lateral deflection. However, the dynamic analysis showed significant lateral force of 450 kN acting on the hole-opener. A consequent bending moment of 120 kNm was acting on the assembly. This explains the twist-off experienced and severe damage to the hole-opener tool itself.

Interestingly, the drilling conditions in the wells were stable except while drilling through the Utsira sandstone in the lower part of the holes section. Because this formation is loose, unconsolidated sand and the upper part is in hard formation, the torsional and lateral vibration levels had increased significantly. A similar but opposite response was found drilling out of the formation into the underlying shale where vibration levels gradually started to drop until all stabilizers exited the sand. The problem was caused by fluid and mechanical erosion of the wellbore wall. Consequently, stabilization was reduced and stabilizer blades dug into the side wall which further increases side load. It was also found, that vibration levels increase as soon as the bit enters the Utsira sandstone without any change in operational parameters.

It was found out that PDC provided higher ROP but it excited a higher vibration levels. Because of the stick-slip risk, roller cone bit was chosen for drilling. Another problem occurred while drilling. Because there was no sign of lateral vibration in the shale, the rotational speed was optimized for hole cleaning. But when the drilling of the sandstone started rotational speed was decreased significantly in order to minimize vibrations. Consequently, the hole cleaning efficiency decreased but it was still sufficient to provide adequate cleaning. Unfortunately, it can be seen that with optimizing one paramater we affect the second one.

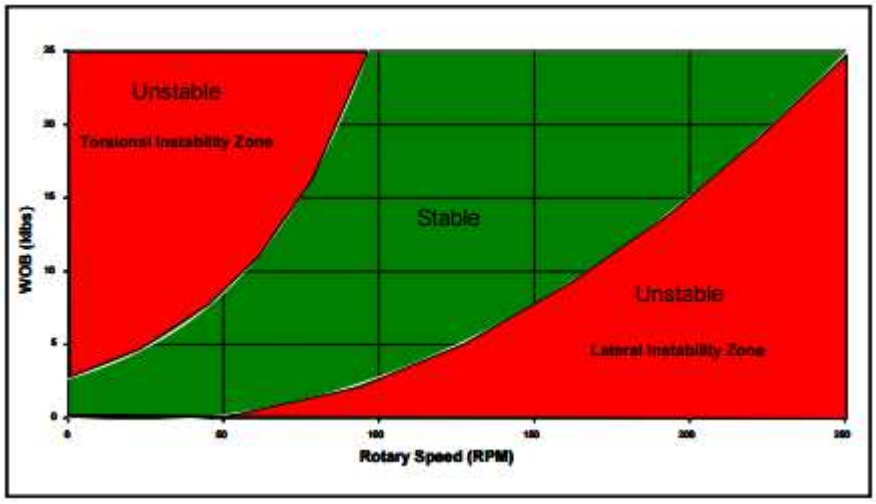

Figure 20: RPM vs. WOB stability diagram for drilling 24 inch well through the sandstone developed by Elsborg et al. (2006).

The study confirmed that a detail analysis and plan are the right approach. In comparison to an offset well, the optimized well shows that optimal drilling parameters and BHA design can significantly reduce vibration levels and avoid a potential RSS tool failure. Additionally, stability diagram was developed, as seen in Figure 20. Such a detailed planning gave the team substantial improvement in performance and saved costs. Consequently, the well accuracy was as planned, without any deviations.

The study confirms that drilling dynamics is highly dependent on the formation drilled. In this case combination of sandstone, claystone and shale caused higher vibrations. In the figure below the authors developed how to adjust operational parameters to mitigate severe effects of drilling dynamics.

Lithology	RPM	Comments
Nordland Claystone / Siltstone (above Utsira)	130	RPM – hole cleaning
Utsira Sand	80 - 120	RPM – reduce vibration
Massive Utsira Sand	80 - 110	RPM – reduce vibration
Between Massive Utsira Sand and Top Hordaland	Claystone: 130 -140 Sand: 80 - 110	Actively adjust RPM using real-time dynamic measurements while drilling interbedded claystone and argillaceous sands
Hordaland Claystone	130 - 150	RPM – hole cleaning

Figure 21: RPM adjustment while drilling 24 inch hole.

3.2.8 The case studies summary and lessons learned

If all the case studies are summarized as in the Table 5, one can observe a few interesting facts. The first one is that the biggest issues occurred in relatively big holes ranging from 12 inch to 24 inch. These data confirm the statement that severe vibrations are more likely to appear in bigger wellbores. Another significant observation is that all the failures were very costly and they resulted in increased non-productive time. Therefore, the phenomena should always be taken into account in order to prevent unnecessary damage to the equipment or even personnel. The main reason why the case studies above were included in this work is that they recognized the issues, analysed them and solved them. It can be observed that in all the studies monitoring was implemented. It follows that monitoring is a starting point to recognize and evaluate issues. After the issues were found an in-depth analysis was done in order to gain more knowledge about them. During this process solutions were proposed and some, rather radical, changes were made. In conclusion, the failures were mitigated, costs and NPT reduced, and target depth was reached faster with less or zero incidents.

Table 5: The case studies summary.

	Ramizer et al., 2010	**Mason et al., 1998**	**Bailey et al., 2009**	**Elsborg et al., 2006**
Location	Mexico	Mobile Bay	/	Norway
Borehole	17-1/2”	/	12 ¼” motor	24”
Formation	From soft shale to abrasive and high strength sandstone	From soft chalk to strong limestone	Interbedded sands and shales	From hard formation to loose; sandstone and from shale to sand
Issues	NPT up to 19 days, tool failures, high lateral vibrations	Washout hole, tools failure	Roller reamers breakage, MSE readings above 100 ksi	Hole opener failure, string twist off, fishing trips
Solution	BHA redesign, powered RSS (mudmotor + RSS)	Anti-whirl measures	BHA redesign	Detail analysis, optimal drilling parameters,

				BHA redesign.
Improvement	100% ROP improvement Lat. Acc. Decreased 50% TD reached 28 days faster	Failure rate dramatically reduced	Cracking reduced to 0. 36% ROP increase	Accurate, reduced vibrations, no tool failures.

4 EXPERIMENTAL SETUP

The previous chapters describe how to gain geomechanical information, why the information is important and what their effect on drilling dynamics is. In this chapter, the experiment procedure will be described. Objectives of the experiment are to derive uniaxial compression strength with a help of empirical correlations which use sonic velocity or porosity as input parameters. Only UCS is derived in the experiment. Therefore, destructibility (not friction, for instance) of a rock is used as the parameter, which would help us to understand vibrations severity. If additional properties are known, such as formation dip, then occurrence of severe vibrations can be evaluated easier. Sandstone and limestone samples were chosen for the experiment. They were chosen because they both have high strength, which means there is a potential for severe vibrations while drilling through one of them within a soft formation. These two types are also common worldwide, thus likelihood to drill through this type of formation is high.

4.1 DESCRIPTION OF THE SAMPLES

Limestone

Limestone is a common sedimentary rock composed primarily of mineral calcite and aragonite. Both of these minerals have the same chemical composition ($CaCO_3$) but different crystal forms. Limestone represents approximately 10 % of all sedimentary rocks. Biochemical limestone is formed from the fragments of the marine organisms including foraminifera, corals, clams, and many other microscopic organisms. These organisms have shells made up of calcite or aragonite and when these organisms die, their shells settle at the ocean floor where these are compacted and cemented together to form limestone. Limestone can also form chemically when calcite precipitates out of oversaturated solutions.

Besides calcium carbonate limestone also contains “detritus” which is a material comprised of sands and muds that are excreted by the organisms, have fallen off higher parts of the seabed, or have eroded off the land in rivers. This detrital material gives limestone its color i.e. grey or brown etc. (Pettijohn, 1983)

Limestone is easily soluble in water and weak acids, therefore most of the world’s natural caves and karst topographies are formed in limestone deposits. Limestone gives strong effervescence upon reaction with dilute HCl, which is very important parameter in identification of limestone. It is estimated that about 50% of world’s oil and gas reserves are contained in limestone buried beneath the surface. (Moore, 2013)

A limestone sample from a quarry was acquired. It is from the Triassic period and formed in the Alps. It is most probably formed in the Limestone Alps, which are a mountain range system of Alps in central Europe. These systems are in three main groups namely, Southern limestone Alps, Northern limestone Alps and Western limestone Alps. Unlike the central Alps, which are composed primarily of crystalline rocks, the Limestone Alps have light colored limestone. Besides limestone it contains dolomite, marl and sandstone as well. This means that the rock is relatively young. It contains around 55 % of CaO. Similar limestone deposits are found worldwide in abundance on all continents. World's largest limestone quarry is located near Rogers City, Michigan, USA.

Figure 22: The overcored limestone sample which was used in the experiment.

Limestone often emerges from earth surface as rocky outcrops. Numerous examples of such topography are present worldwide. Examples include Malham Cove in North Yorkshire England; on Fårö near the Swedish island of Gotland the Burren in Co. Clare, Ireland; the Verdon Gorge in France; and the Isle of Wight, the Ha Long Bay National Park in Vietnam, the Niagara Escarpment in Canada/United States, Notch Peak in Utah, and the hills around the Lijiang River and Guilin city in China. Limestone exhibits extremely level expanses and an excellent example of such expanse is in Europe is the Stora alvaret, Sweden. Today limestone is being deposited in various environments across the globe. Most of these limestone forming environments are located in shallow water areas between 30 degree north latitude and 30 degree south latitude. Limestone is forming in Caribbean Sea, Gulf of Mexico, around Pacific Ocean, Indian Ocean, Persian Gulf and within the Indonesian Archipelago. Bahamas platform located in Atlantic Ocean is producing an extensive limestone deposit. (Ahr, 2008)

Due the complex nature of interaction between various parameters, such as porosity, permeability and fluid mechanics, in carbonate rocks, it is very difficult to predict the nature of the reservoir. Limestone and other carbonate rocks are proven to have excellent reservoir

potential (Moore and Williams, 2013). A significant amount of world's petroleum reservoirs are found in carbonate rocks. One of the largest oil field in Saudi Arabia, Ghawar oil field, has a reservoir in carbonate rocks. Other major carbonate reservoirs of the world are located in Middle East, Libya Russia, Kazakhstan and North America.

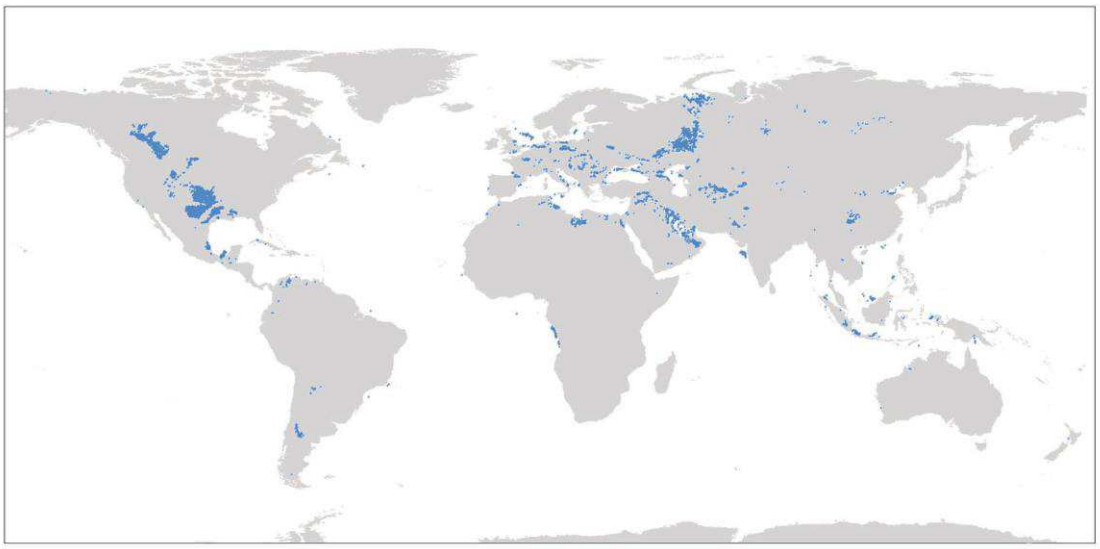

Figure 23: Carbonate reservoirs around the world. (Ehrenberg et al., 2005)

Figure 24: The broken part of the limestone sample. Foliation where the sample broke is clearly visible.

Sandstone

Sandstones are classified as rocks with clastic origin. Like any sedimentary rock, their formation consists of cemented grains which can be fragments of pre-existing rock or be mono-minerallic crystals. The most common grains which bind the cements together are calcite, clays and silica. Geological range of grain sizes is between 0.0625 mm and 2 mm. Environments where sandstone can deposit is split between terrestrial environments such as

rivers, alluvial fans, flacial outwash, lakes, desserts and marine environments like deltas, beach, tidal flats, turbidites. (Fichter, 2000)

Sandstone is one of the most common sedimentary rocks and is found in all major sedimentary basins of the world. Sand grains show excellent porosity and due to this property sandstone, underneath the surface, can act as an aquifer for ground water and when in depth it can be an excellent reservoir for petroleum. Sandstones are made of several fragments which can be classified into (Boggs, 2000):

- Quartz framework grains are the dominate mineral in most sedimentary rocks.
- Feldspathic framework grains are the second most abundant minerals in sandstones.
- Alkali feldspar.
- Lithic framework grains, where clasts of volcanic rocks represent the most common one.
- Accessory minerals such as muscovite, biotite, olivine, pyroxene and corrundum.

All these minerals are bound together with cement. Most common cementing minerals are silicates and calcite.

The sample sandstone used in this research has arenite matrix, which means that it is a very clean sandstone and has very little matrix. The size of grains is between 0.1 and 0.2 mm with a cylindrical shape.

Figure 25: The overcored sandstone sample which was used in the experiment.

Sandstone is an excellent reservoir rocks and most of the oil fields in the world have sandstone as reservoir. Over 60% of world's giant oil fields have sandstone as reservoir rocks. This quality is due to the fact that sandstone has high porosity and high permeability, but these two depend upon environment of deposition and post depositional processes like cementation and compaction (Pettijohn, 1983). One of the world's largest oil field, Burgan oil

field, has a sandstone reservoir. Below is a figure showing the geographical distribution of sandstone across the world (Ehrenberg et al. 2005). From the map it can be seen that sandstone reservoir are more common than carbonate reservoirs.

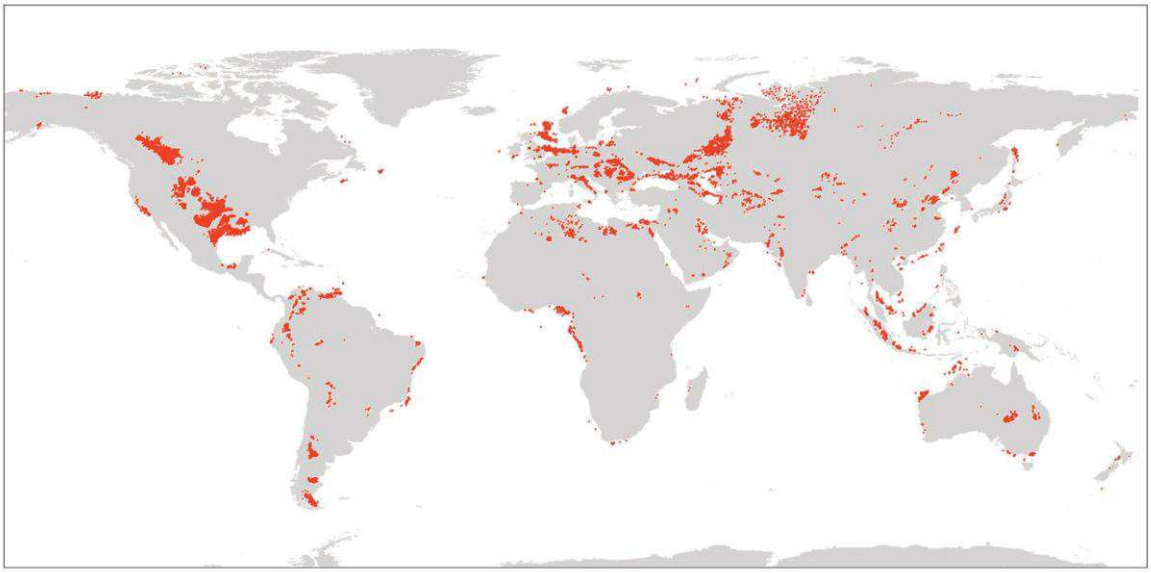

Figure 26: Sandstone reservoirs around the world. (Ehrenberg et al., 2005)

A laboratory analysis was done from in the quarry where we got the sample. Mineral composition is as presented in the table below. Additionally, 53.7 % of calcite and 4.1 % of dolomite was found in the sample. The abundance of calcite in the sandstone can be attributed to the late diagenesis which resulted in the precipitation of calcite as cement. This cementation caused the reduction in porosity and hence the permeability of the sandstone.

Table 6: Mineral composition of the sample sandstone.

Mineral	**Percentage**
Quartz	20 - 25
Rock fragments	10 - 15
Carbonates	55 – 60
Feldspars	traces

Several tests were done in the quarry where this rock was acquired. The tests and their results are as follows:

Table 7: The tests that were done on the sandstone formation from where the sample was taken.

Test	**Result**
Density	2640 kg/m^3
Porosity	3.6 %
UCS (dry)	188 MPa

UCS (saturated)	155 MPa
Bending strength (dry)	20.2 MPa
Bending strength (saturated)	8.0 MPa
Heat extension coefficient	0.0097 mm/m°C
Thermal conductivity	1.1 W/mK
Young's modulus static E_s	40541 MPa
Dynamic longitudinal modulus E_D	51579 MPa
Dynamic Poisson's number	0.14

The sizes of both samples were also measured, as seen in the table below:

Table 8: Size of the samples.

Sample	**Length**	**Diameter**
Limestone	6.90 cm	4.98 cm
Sandstone	11.30 cm	5.46 cm

4.2 MEASUREMENTS DESCRIPTION

4.2.1 Ultrasound and porosity measurements

The ultrasound and porosity measurements were done at Geophysical Department at University of Leoben. The measurements were done for both the limestone and sandstone sample. Primary or compressive wave velocity and porosity according to Archimedes principle were measured. Ideally, the shear (or secondary) wave velocity would be also measured. However, because samples for this measurement need to be very small (maximum diameter of 2cm), this measurement was not done. The experiment procedure will be described in the next paragraphs.

Already prepared samples were put into the ultrasound measurement cell. The cell is connected with probes to the sample and further to an ultrasound generator. For a better coupling the probes are connected to the sample at axial pressure of two bar. One probe represents transmitter and the second one is receiver. Geotron USG 40 (from Germany) ultrasound generator was used. With the ultrasound generator a Dirac impulse is sent to the transducer and results in a mechanical pulse travelling through the sample at certain frequency. The frequencies which can be generated with this device are as follows: 20, 46, 64, 80, 250 and 350 kHz. The arriving signal is shown on the computer screen with a storage

oscilloscope. Because of time lag, all the measurements are dead time corrected. Probes show a primary low amplitude onset, which is referring to the compressional wave (Gegenhuber, 2016). This generator can be used in a laboratory as well as in the field.

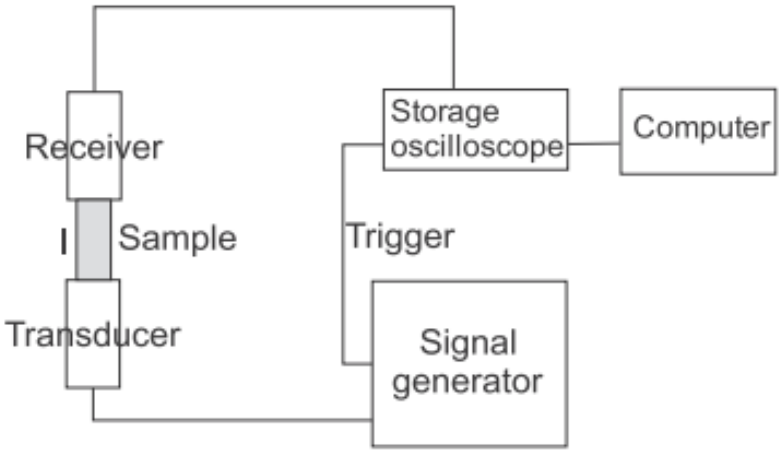

Figure 27: A schematic view of the ultrasonic device. (Gegenhuber, 2015)

In the figure above a schematic view of the setup can be seen. The real setup can be seen in the figure below. Probes (receiver, transducer), the sample and generator are seen in the figure.

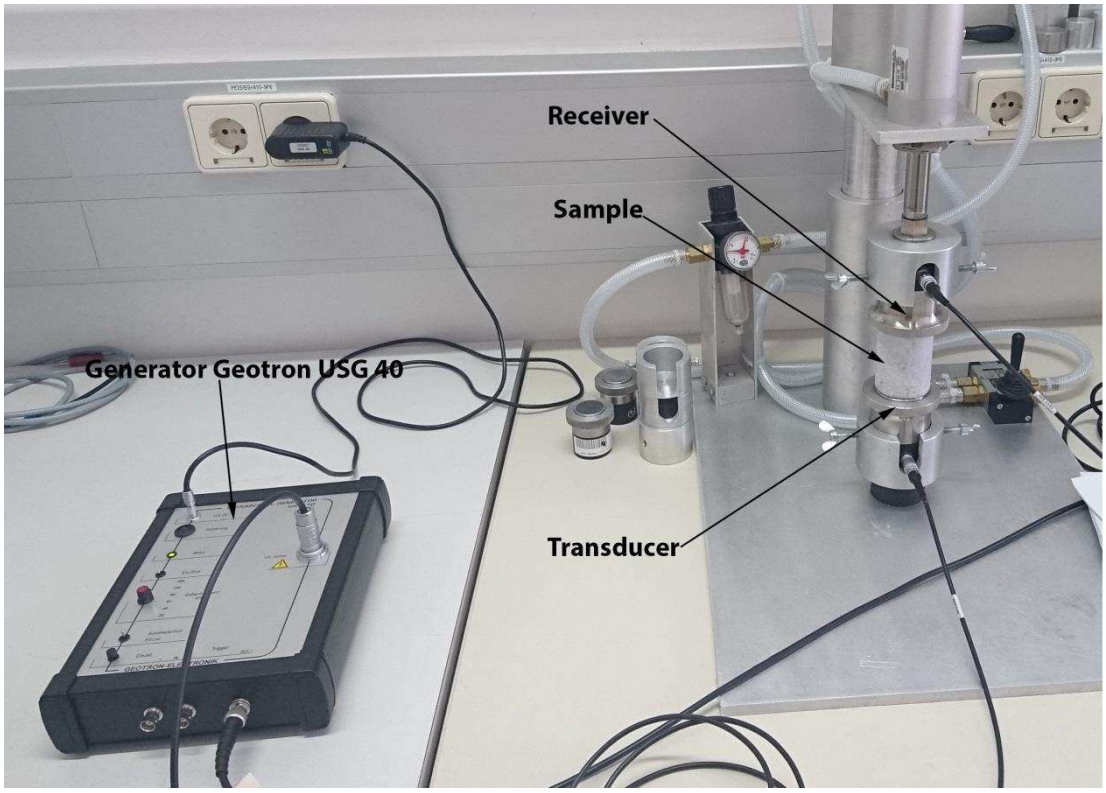

Figure 28: The experimental setup; Generator Geotron USG 40, receiver, transducer and a sample.

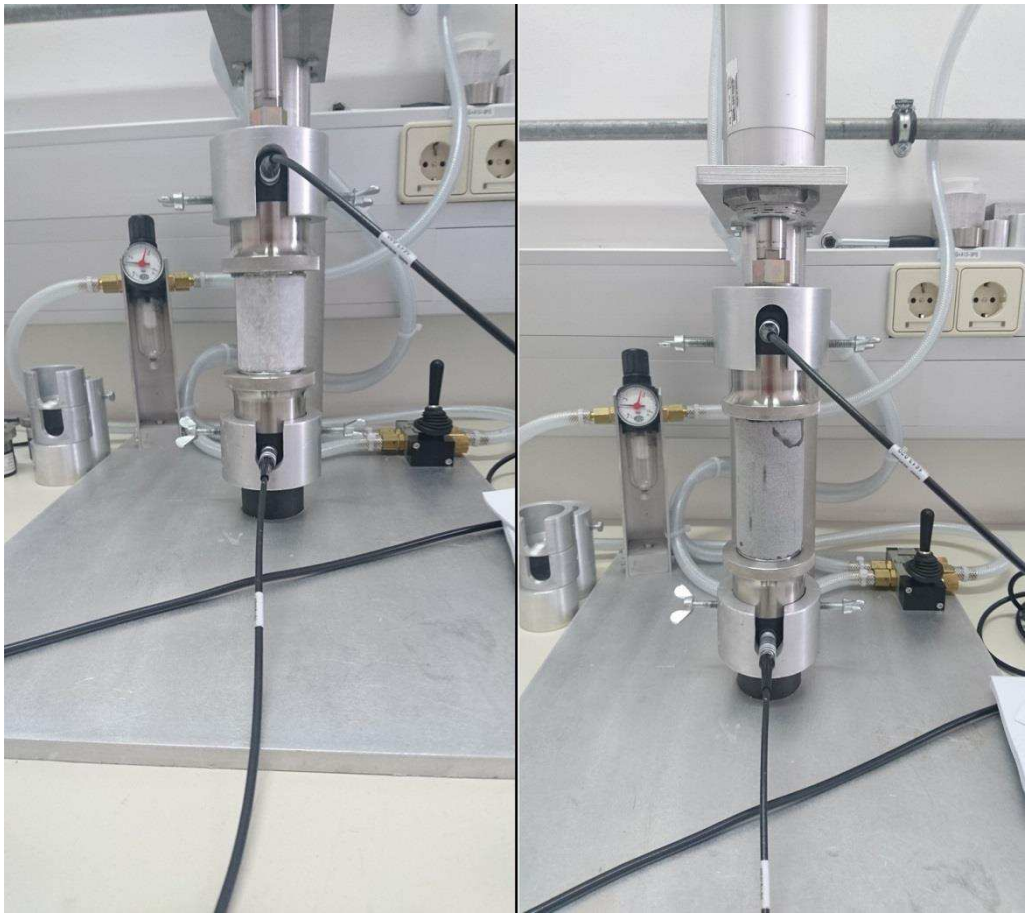

Figure 29: Limestone (left) and sandstone (right) sample in the measurement cell.

The plan of the thesis was that acoustic velocities are measured and porosity from a log obtained. In the best case scenario, a density log tool would be used. This would allow us to simulate the field measurement. However, there was no chance to use density log since this is a borehole measurement and is therefore not available in the laboratory. As an alternative, porosities were measured by Archimedes principle. These porosities will be used as if they were derived from the density log in field. They were measured by the following procedure:

1. A dry sample mass (m_d) is first determined.
2. A sample is immersed into a liquid and then a saturated mass (m_s) is measured.
3. A sample mass under buoyancy (m_b) is obtained.

After all of the above masses are determined, porosity can be calculated with the following equation:

$$\emptyset = \frac{m_s - m_d}{m_s - m_b} \tag{55}$$

4.2.2 The UCS test procedure

A UCS test was done in Subsurface Engineering Laboratory at University of Leoben. In this chapter general test procedure will be briefly described.

UCS or unconfined compression test is a simple laboratory testing method to assess the mechanical properties of rocks and soils. As a result, it provides stress-strain characteristics of the rock or soil. It is routinely used in all geoscience industries. (Bardet, 1997)

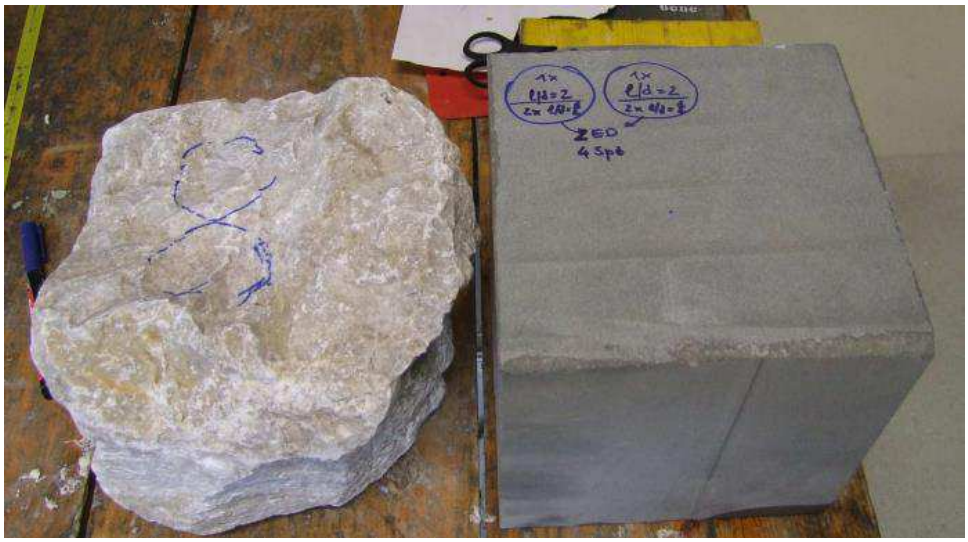

Figure 30: The rocks from which the samples were cored.

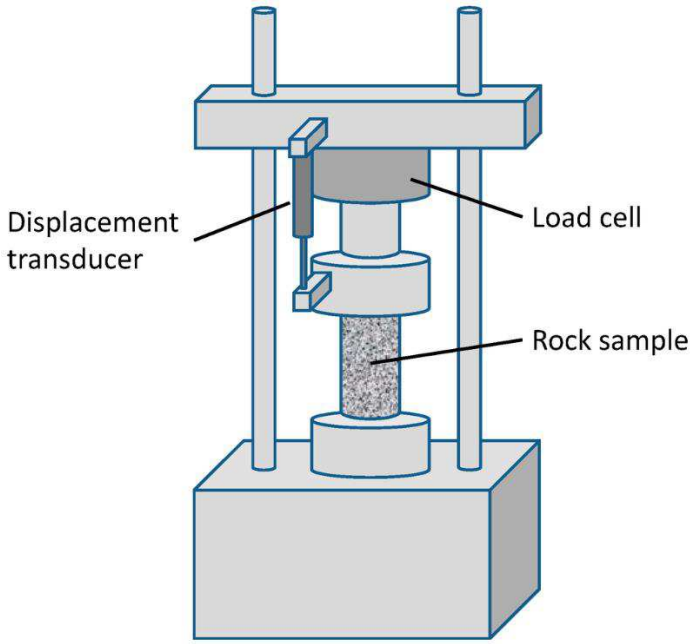

Figure 31: A typical setup for uniaxial compression test. (Mwanga et al., 2015)

Prior performing the test, the sample must be properly prepared. If we are sampling soil a cylindrical tube is used and if we are sampling rocks an over-coring operation must be done. The diameter of a sample should be taken according to the expected strength and our machine maximum available force. The strength can be assumed according to experience and similar rock types. The maximum force is a parameter and is stated on the machine itself. Ideally, the sample should have length-to-diameter ratio on the order of two. When the sample is prepared, it can be loaded into the cell, as seen in the Figure 32. Finally, the loading can start. The loading is continued until the sample develops an obvious shearing plane, which is the case when soil is tested, or the deformations become excessive, which is the case when rocks are tested. The loading is added in increments which result into a stress-strain relation. Dimensions of the sample must be corrected for each increment, because they change with increased force/pressure applied on it. The maximum load per unit area is defined as the unconfined compressive strength. Afterwards, a stress – strain graph can be shown. The maximum pressure is easily seen on the stress – strain curve. (Bardet, 1997)

Sample size and overcoring

Because of different strengths and the machine specifications, it is important to determine the size of the specimen prior overcoring. It was fairly easy in this case, because we did approximately know what strength to expect. First, if we take diameter of the specimen of 2.5 cm, then the area of the cylinder is around 4.9 cm^2. If the strength of the sample is expected to be around 200 MPa, then the force should be as follows:

$$F = \sigma A = 200\ MPa * 4.9\ cm^2 = 98\ kN \tag{56}$$

The calculated force is easily achievable with the compression machine. Because it is recommended to take a bigger sample, we should try to calculate force in the case of 5 cm diameter:

$$F = \sigma A = 200\ MPa * 19{,}6\ cm^2 = 392\ kN \tag{57}$$

As the force in this case is still well below the maximum applicable force of 2400 kN, we decided to core 5 cm diameter specimen. Due to coring operation the diameters slightly differ, as seen in the Table 8. One of the benefits to core a bigger specimen is that it has bigger mass which results in more accurate stress-strain relationship. The question appears why not to core even bigger diameter then. The answer to this is that bigger diameters require longer samples, which is usually hard to achieve due to foliations or faults. Therefore, the same diameter was used for the second sample. As mentioned earlier, diameter to length ratio should be two, which results in 10 cm long specimens. Unfortunately, the limestone specimen broke during the process due to a foliation structure (it would be impossible to core even bigger diameter).

Because of the breakage, the length of the specimen is approximately 6 cm. The rocks from which the samples were cored can be seen in the figure 30.

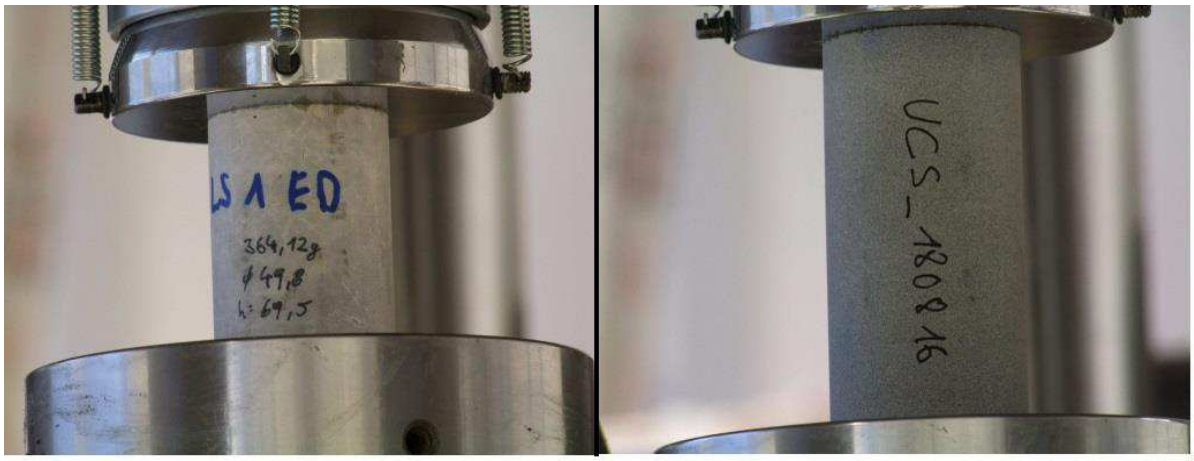

Figure 32: Both samples loaded into the cell; limestone (left) and sandstone (right).

5 RESULTS AND DISCUSSION

5.1 EXPERIMENTAL RESULTS

5.1.1 Ultrasound measurements

Results for primary wave velocities and porosities are given in the table below.

Sample	V_P [m/s]	Porosity [%]
Limestone	5714	0.68
Sandstone	5159	1.9

5.1.2 The UCS tests

The UCS test results are presented in this chapter. As a result of the test, force – strain graph, time of the test and broken sample are presented.

UCS test of the limestone sample

First, a graph showing the force applied versus time of the test. The sample was gradually loaded with a force rate of 120 kN per 60 seconds. The total duration of the test was 161 seconds and the maximum applied force, as seen from the graph, was 250 kN. This is the force, where the sample broke. The second graph, which can be seen in the Figure 34, shows the typical force – strain relationship. Since the sample's diameter is known, it is not hard to calculate maximum strength. The UCS strength of this sample is as follows:

$$UCS_l = \frac{F_{max}}{A} = \frac{4 \cdot 250\ kN}{\pi(4.98cm)^2} = 128.89\ MPa \tag{58}$$

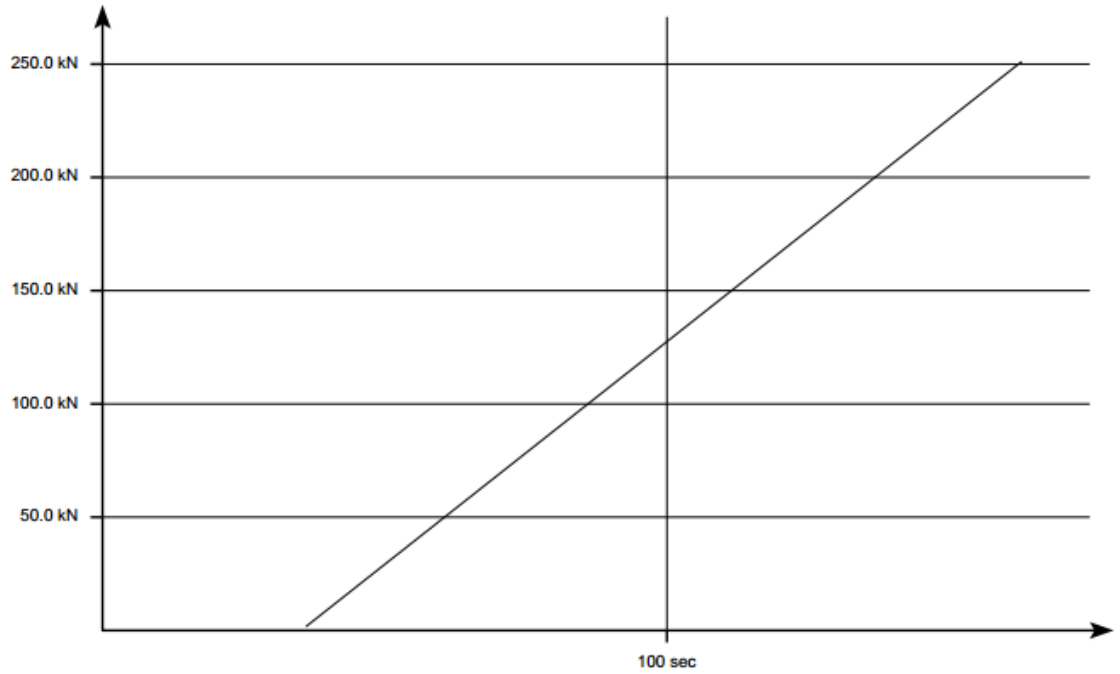

Figure 33: Duration of the UCS test, when limestone sample was loaded.

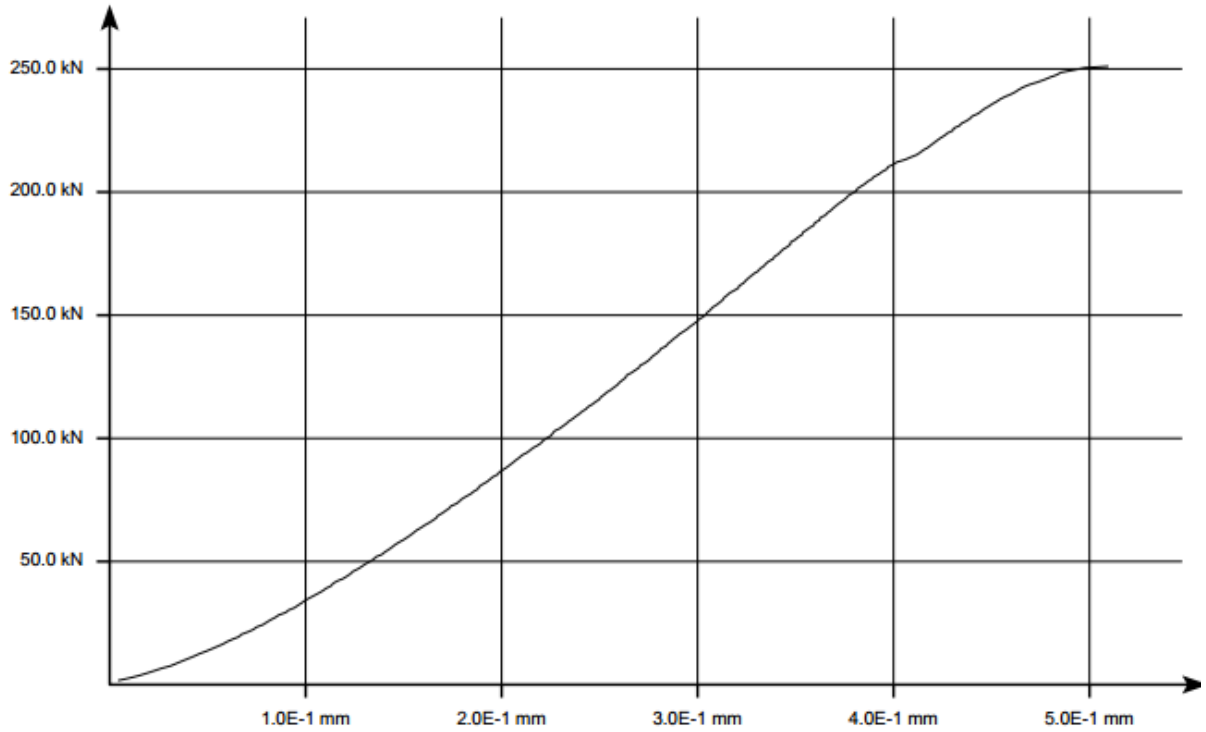

Figure 34: Force - strain curve for the limestone sample.

It can be seen that maximum strain of the sample was 0.5 mm. From that it follows, that the rock is very brittle, but it also has relatively high strength. The breakage of the sample can be seen in the Figure 35.

Figure 35: The limestone breakage.

UCS test of the sandstone sample

The same procedure was done for the sandstone sample. This sample was expected to have higher strength. Therefore, the loading rate was higher at 125 kN per 60 seconds. Total duration of the test was 213 seconds and in the sample broke at 417.5 kN.

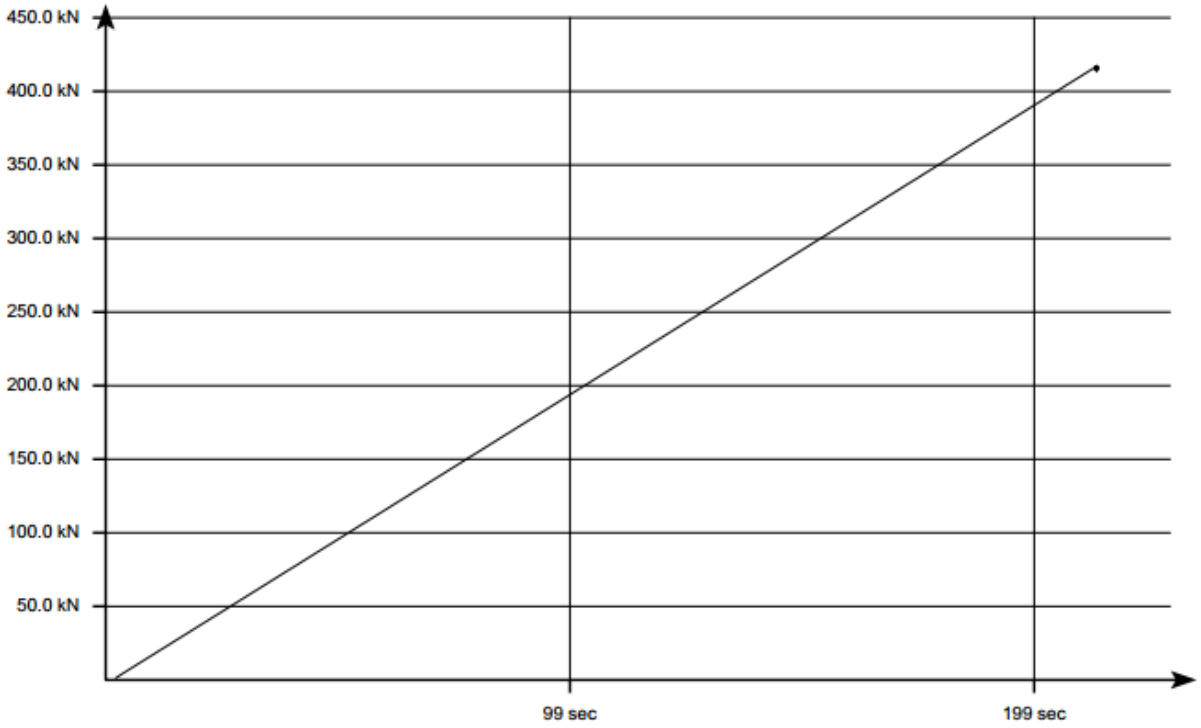

Figure 36: Duration of the UCS test, when sandstone sample was loaded.

If maximum force and diameter of the sample are known, the maximum strength can be calculated, which yields:

$$UCS_s = \frac{F_{max}}{A} = \frac{4 \cdot 417.5\ kN}{\pi(5.462\ cm)^2} = 178.22\ MPa \tag{59}$$

The maximum strength is for approximately 50 MPa higher than the one of limestone. The maximum strain is 1 mm, which means that this sample has brittle characteristics as well. The breakage of the sample released a lot of stress, which resulted in splitting the sample, as seen in the Figure 38.

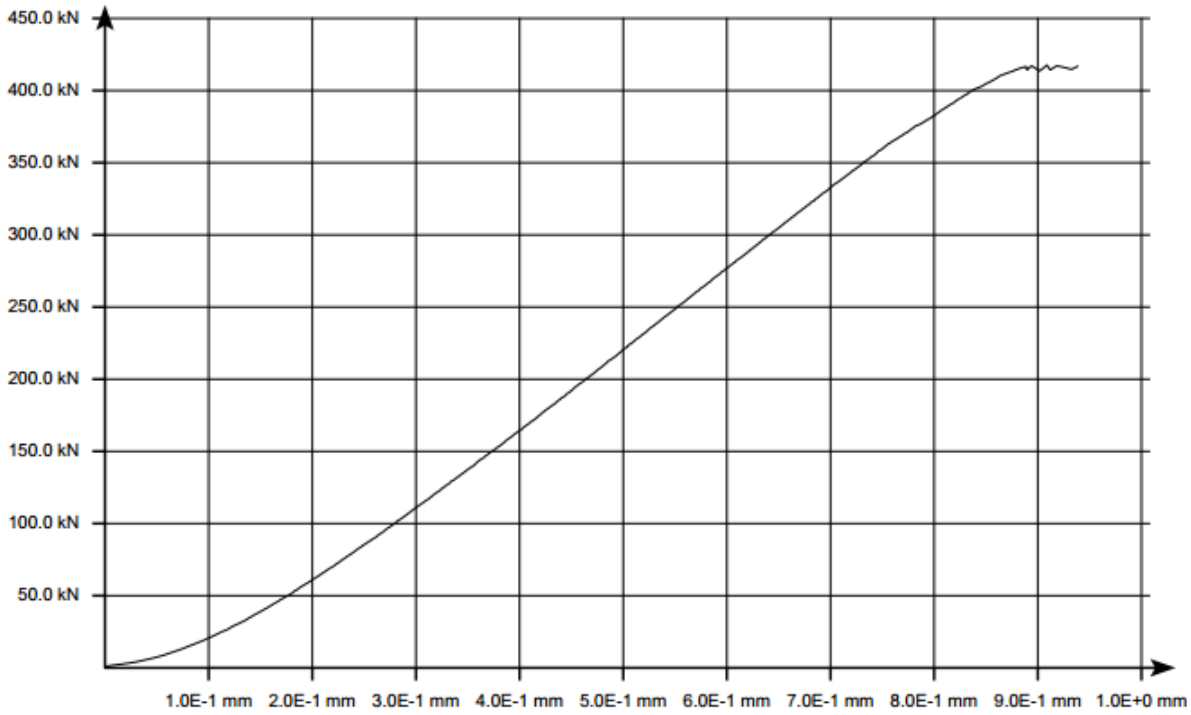

Figure 37: Force - strain curve fort the sandstone sample.

Figure 38: The sandstone breakage.

5.1.3 Comparison of the correlations with the UCS test values

Now when all the experiments are done and all data available, comparison between the laboratory values and empirical values can be made. First, calculated correlations with laboratory measured wave velocity and porosity are given, as seen in the table below.

Table 9: Empirical correlations based on sonic velocity and porosity for the sandstone sample..

	Correlation name	UCS value [MPa]	Calibration factor
Sonic velocity	Freyburg 1972	149	1.20
	Raeen et al. 1996	45	3.90
	Moor et al. 1999	102	1.75
	Rahman et al. 2010	58	3.08
	Chang et al. 2006	160	1.11
Porosity	Vernik et al. 1993	229	0.78
	Edlmann et al. 1998	123	1.44
	Farquhar et al. 1994	208	0.86
	Sarda et al. 1993	290	0.61
	Chang et al. 2006	229	0.78

The Table 10 shows empirical correlations for the limestone sample. Unfortunately, there are not as many as for sandstones.

Table 10: Empirical correlations based on sonic velocity and porosity for the limestone sample.

	Correlation name	UCS value [MPa]	Calibration factor
Sonic velocity	Chang et al. 2006	135	0.95
	Golubev 1973	200	0.61
	Militzer 1973	58	2.20
Porosity	Farquhar et al. 1994	174	0.74

After the results above, it can be seen that calibration factors vary significantly. Therefore, the correlations should be used with care and according to the procedure, which is described in the next chapter. Raeen et al. 1996, Rahman et al. 2010 and Militzer 1973 correlations are not recommended for use in this case. They were used to show how big the differences can be. However, Chang et al. 2006 correlations prove to be the best ones and need calibration factors of 1.11 and 0.95 for sandstone and limestone, respectively. This proves that high number of tests on different samples yield the best result. Moreover, it can be seen that porosity correlations usually overestimate the real value, whereas sonic velocity correlations underestimate the real value.

5.1.4 Process of obtaining rock properties from logs

After the experiments, extensive literature review and comparison were made, a flow chart showing the process can be given. The flow chart is shown in the figure below. Two flow charts were made; one for a new field, where number of coring samples are limited and the second one for a new field, where numerous coring samples are available. The differences between the two will be expressed in the next paragraphs.

Figure 39 shows the second example, where numerous coring samples are available. Like in any operation, drilling to the section of interest is the first step. Second, coring of the formation should take place and, ideally, several samples within one formation are taken. The best diameter size would be around two inches with a four inches length. If ten samples are taken, the core should be around 40 inches long (around 3.5 feet), which usually should not be a problem. Next, if LWD is used then log data are already available and conventional logging is not needed. If no, then logging to the end of formation is conducted. The most important logs (rock properties wise) are sonic, density and gamma ray. After porosity values, travel times or gamma ray radiation are measured, values, marked as y in the figure, are derived. It is important to correlate these values with coring depth and correct them if necessary.

When the cores are acquired and properly cut, analyses in a laboratory can be done. First, non-destructive analysis such as hardness, porosity, permeability and others are made. Second, destructive tests like UCS or elastic moduli (Young's modulus) test can be conducted. The values derived from these tests are marked as x values in the figure.

When the above procedure is done, principle of linear correlations is applied, described in the chapter 2.5. As a result, a correlation between a log measurement and lab value is obtained. Correlations can be between UCS and travel time, UCS and porosity, UCS and Young's modulus (derived from logs), to name a few.

The second case, where coring samples are limited, is shown in Figure 40. Like in the first case, first drilling to the formation of interest should be done. Second, coring should also be done with at least one sample retrevied. Afterwards, different logs such as density, sonic or gamm ray log, can be run. After logs are run, it is important to correlate coring depth with logging depth. It should be corrected if necessary. Another parameter, which should be checked, is critical porosity. Porosity should be checked in a laboratory. If porosity is higher than critical porosity then correlations should not be used due to incorrect acoustic values. However, if porosity is below critical porosity value then predominant lithology should be determined. It can be done with logging help as well as in a laboratory (XFD analysis for instance). Four possible outcomes appear after the analysis:

- If volume of sandstone is higher than volume of clay, limestone or dolomite, then UCS correlation for sandstone should be used.
- If volume of clay is higher than volume of sandstone, limestone or dolomite, then UCS correlation for shale should be used.
- If volume of limestone is higher than volume of clay, sandstone or dolomite, then UCS correlation for carbonates (limestone) should be used.
- If volume of dolomite is higher than volume of clay, limestone or sandstone, then UCS correlation for carbonates (dolomite) should be used.

If there is none of this lithology present, then the correlations should not be used.

After a correlation is used, other parameters can be calculated, if needed. Furthermore, laboratory tests on at least one core should be done. When laboratory values are known, they can be compared with empirical values. In the comparison, the empirical values should be calibrated according to tested values. After this is done, a calibration factor should be applied and the correlation can be used for other wells within the same field.

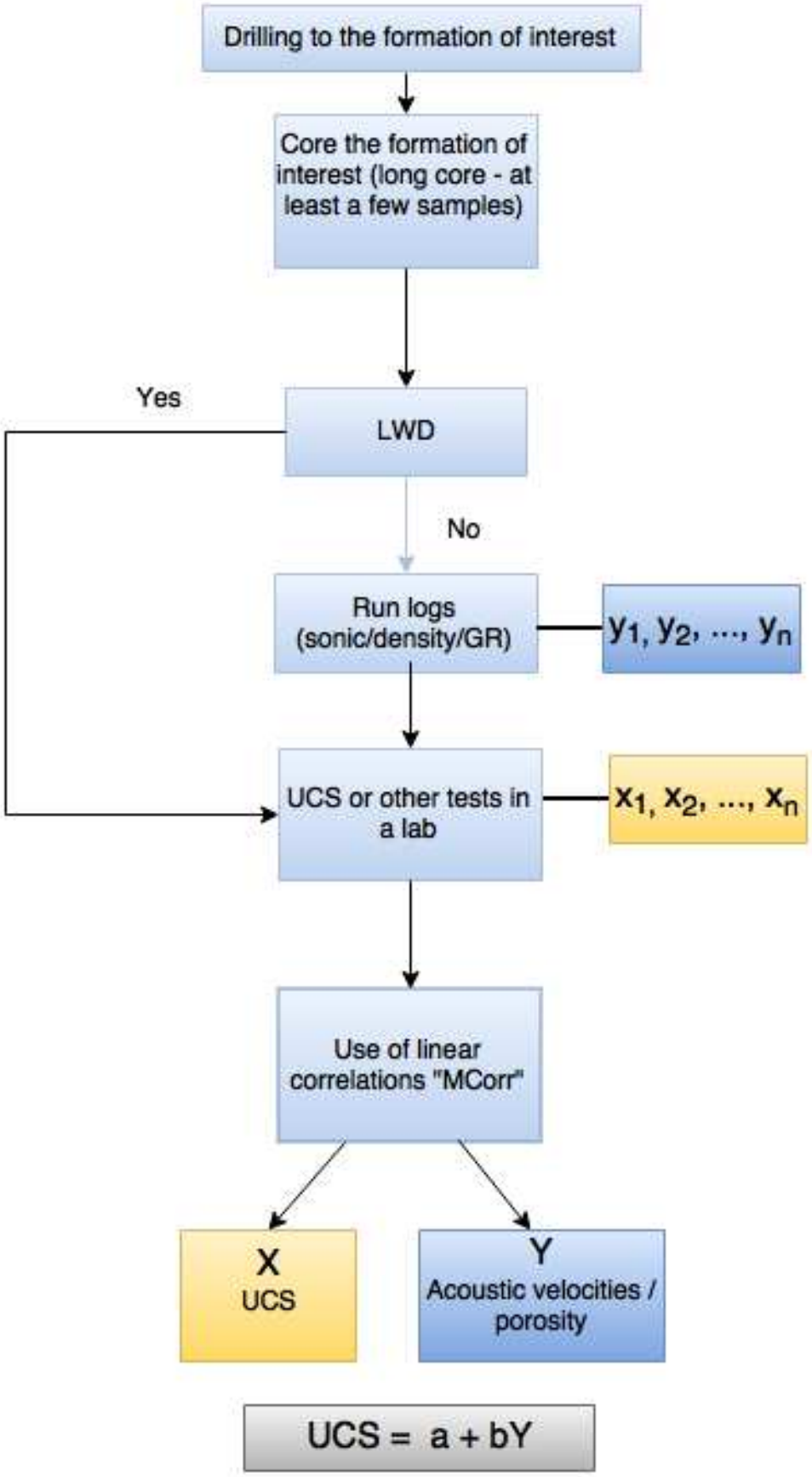

Figure 39: A flow chart showing the procedure of obtaining rock properties in a new field with numerous coring samples available.

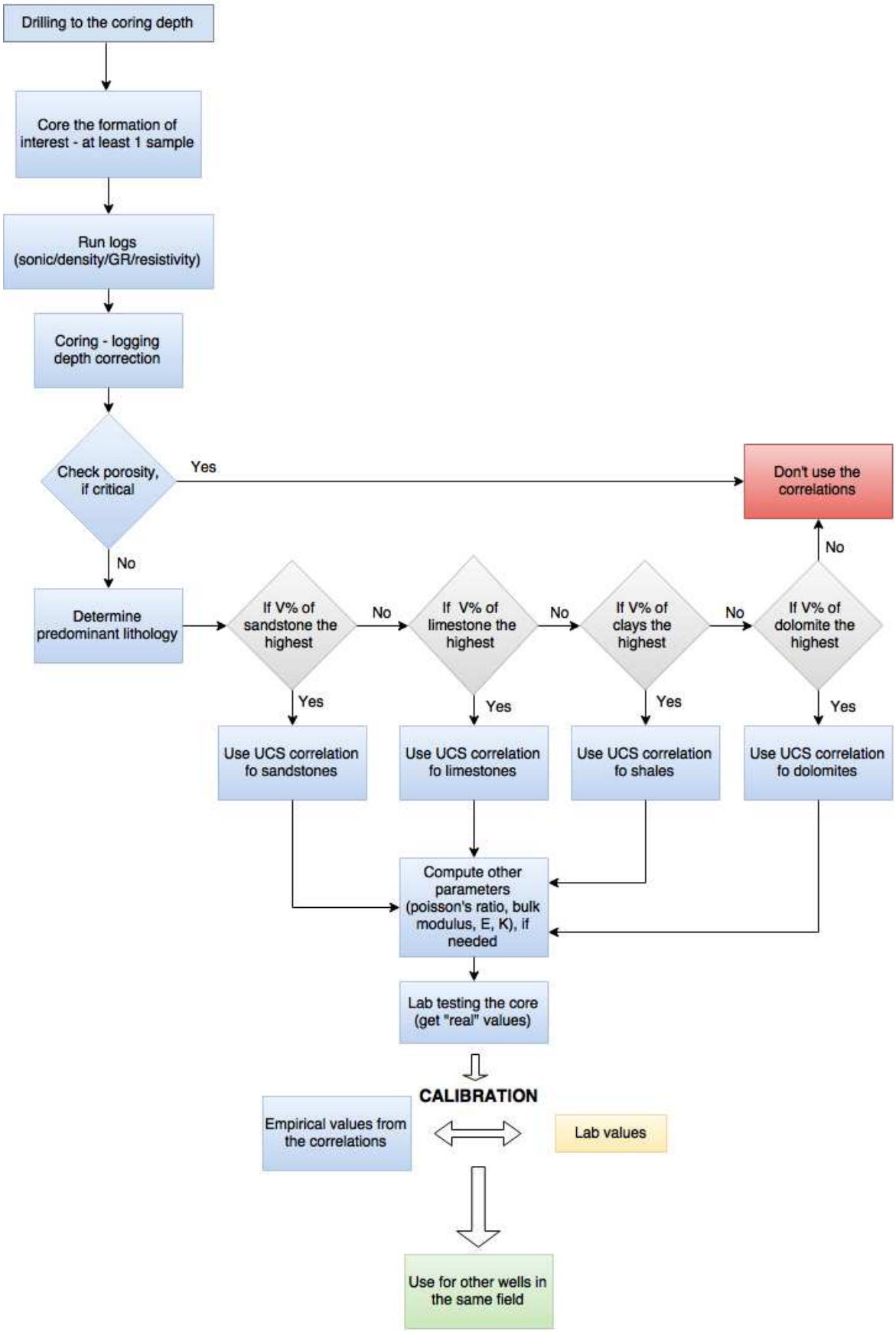

Figure 40: A flow chart showing the procedure of obtaining rock properties in a new field with limited coring samples available.

5.1.5 Advantages and Disadvantages of Obtaining Rock Properties from Logs

There are numerous advantages using the method described in the previous chapters. Some of them are:

- It is very cost effective; it can save up to 70 % of resources compared to conventional coring and laboratory testing. UCS and laboratory tests which obtain rock properties are usually costly and time consuming. A problem is that such laboratory is usually not in field. Therefore, samples are transported to the location, which makes the process even more time consuming.
- If LWD is used, this method can provide real-time information about rocks. This makes it very attractive for all other analysis such as drilling dynamics.
- A continuous profile can be made with this method. It means that there is more information about longer sections, than just those which are cored.
- It can be used in wells, which are not planned to be cored. Additional information is therefore available.
- The method can be used in field.

However, the method is far from perfect and therefore has several disadvantages such as:

- The accuracy of the empirical values can be questionable due to changing formation composition.
- Sonic and density log are not always used. Therefore, this method cannot be used, except if additional correlations are used to correlate other logs with sonic or density log.
- It does not work for very loose or unconsolidated formations.
- It needs to be calibrated when used in a new field. The problem could be solved with an extra big database of correlated values. However, such database is not available to date.
- Due to low depth investigation of logging tools, the data might not be “real”, especially if mud invaded the near wellbore during drilling operation.

5.2 RECOMMENDED PRACTICES TO AVOID DRILLING DYNAMICS DYSFUNCTIONS

After extensive literature review and analysis of case studies, the best practices to mitigate or avoid drilling dynamics dysfunctions can be given. The recommendations will be given for the most often phenomena which can be encountered during drilling operations. For each phenomenon optimization of surface parameters will be described, potential for damage evaluated and BHA design changes recommended.

5.2.1 Full Stick Slip (FSS)

As described in previous chapters, full stick slip phenomenon can cause a potential damage. On the scale from low to high, the damage can be evaluated as moderate. Nevertheless, it can significantly increase NPT and it can decrease well path accuracy. To mitigate this effect with surface parameters, weight on bit should be reduced and the revolutions increased. Additionally, there are more options if a BHA component or well plan can be changed:

- Friction can be reduced: use of rolling elements, mechanical reduction friction subs, rolling reamers, mud lubrication (use of oil based mud).
- Reduce bit aggressiveness: a short gauge bit is more aggressive and a long gauge bit tends to be less aggressive and create a smoother hole.
- Torque control devices or torque mitigation devices; such as soft torque – the most often used tool for stick slip mitigation. The soft torque is based on an algorithm which counteracts drill string fluctuation. It calculates set parameters for the drive controller.

5.2.2 Low Frequency Torsional Oscillation (LFTO)

Low frequency torsional oscillation is common and as the name suggest they occur at low frequencies which usually do no exceed 100 Hz. Because of low frequencies this effect cannot be mitigated with surface parameters optimization. Additionally, the damage which this oscillation can cause is rather low. A major issue could be that this oscillations lead to fatigue which is very hard to detect. Moreover, increase in torsional rigidity of the BHA or the drillstring would lower the occurrence of this phenomenon. Like in the previous case, torque based surface drive control can slightly reduce the dysfunctions.

5.2.3 High Frequency Torsional Oscillation (HFTO)

On the contrary to LFTO, high frequency torsional oscillation occurs at high frequencies, well above 200 Hz. Previously, it was believed that such oscillation does not exist which led to many unexplained failures. Damage potential for this phenomenon is high. The only surface parameter which can be optimized to reduce the damage is to reduce WOB. Additionally, BHA redesign, bit aggressiveness and torque control should be discussed.

5.2.4 Random Torsional Vibration

A vibration which occurs without any particular pattern or does not follow the phenomena previously described is called a random torsional vibration. This effect can potentially cause

damage, which is usually neither particularly low nor high. It can be classified as medium damage potential. Reducing WOB and increasing RPM would both mitigate the occurrence of this effect.

5.2.5 BHA Whirl

BHA whirl can further lead to other effects, therefore it is important to reduce it in the first place. Similarly, it can be reduced with reduced WOB. A more effective solution would be the BHA redesign which would include friction reducing tools such as rolling reamers and anti-whirl bits. Additionally, use of lubrication is recommended such as oil based mud for instance.

6 CONCLUSION

Comparison of empirical correlations which use sonic velocity and porosity as input parameters to derive uniaxial compressive strength was among other objectives of this thesis. Other objectives include verification of the correlations with an experiment, recommended procedure to use empirical correlations in field and investigation of how rock properties (including formation dip, friction factor and rock strength) affect drilling dynamics behaviour.

The work which was done in this thesis includes an experiment in which sandstone and limestone samples were acquired and UCS, sonic velocity and porosity values were measured. These values were correlated with use of correlations from Farquhar et al. (1994), Militzer (1973), Golubev (1973), Freyburg (1972), Vernik et al. (1993), Sarda et al. (1993), Raeen et al. (1996), Moor et al. (1999), Rahman et al. (2010), and Chang et al. (2006). As a result, a flow chart showing the recommended procedure to use these correlations was made. Additionally, importance of knowing the rocks strength in regard to drilling dynamics was researched.

The scope of this thesis did not include an experiment in which relationship between friction factor and drilling dynamics would be empirically analysed. However, this is a good topic for further research.

The following conclusions can be made:

- The correlations from Freyburg (1972), Vernik et al. (1993) , Farquhar et al. (1994) and Chang et al. (2006) showed the best results.
- The correlations above showed good results, whereas many others like Raeen et al. (1996), Rahman et al. (2010) and Moor et al. (1999) needed calibration factor higher than two which is not acceptable. Many of them work only for certain types of rocks and for certain fields. Therefore, they are very location sensitive.
- Correlations which use porosity as a parameter to derive UCS usually overestimate the real value, whereas the ones which use sonic velocity underestimate them.
- Empirical correlations are limited in use and can only be used for sandstone, shale, dolomite or limestone dominated lithology.
- If the correlation between sonic velocity or porosity and UCS wants to be determined in a field, where numerous coring samples are available, then linear correlations principle should be used, as described in chapter 2.5.
- If the empirical correlations are used in a field, where coring samples are limited, but there is at least one available, then the dominant lithology correlation should be used

and properly correlated with the test value, as described in chapter 5.1.4. Afterwards, the calibration factor should be applied to the empirical values of new wells (within the same field).

- In the future, more cores should be tested. As a result, a bigger worldwide database of correlations would be available. This proved to be true, since the correlation (of Chang et al. 2006) had the largest number of tests on different samples and yielded the best result. However, the problem is that the industry is usually very sensitive when it comes to data sharing.

Drilling dynamics can be studied after BHA design, drillstring configuration, mud properties, operational parameters, hydraulics and rock properties are known. It was found out that rock properties greatly affect drilling dynamics phenomena as well as BHA design. After the analyses the following conclusions can be made:

- Drilling dynamics is a complex topic, which is relatively unknown and undiscovered. Therefore, more research is needed in the future.
- There are four most common phenomena that occur due to vibration: FSS, LFTO, HFTO, random torsional oscillation and BHA whirl.
- A special care about drilling dynamics dysfunctions should be taken because they can increase costs, NPT, tool failures rate and possibility of missing the target.
- The most destructive dysfunctions appear in wellbores with diameter bigger than 12 inches. Transition from soft to hard and abrasive formation is also a perfect environment for higher oscillations. Vibrations reach critical level much higher if there is calcite or sandstone (high UCS rocks) stringer in a soft formation as described in chapter 3.2.7.
- Appropriate measurement system is necessary to detect vibrations. Advanced accelerometers should be used to record frequencies above 200 Hz. After data are obtained, analysis should be done and improvement made, such as BHA redesign, use of lubrication, roller reamers or soft torque system. Additionally, surface parameters could be optimized in order to mitigate the effect.
- Vibrations which occur at higher frequencies are proved to be as hazardous as the ones, which occur at lower frequencies.

7 REFERENCES

Wyllie, M.R.J., Gregory, A.R. and Gardner, L.W. Elastic Wave Velocities in Heterogeneous and Porous Media. Geophysics, 21, 1956, pp 41-70

Raaen, M.A. and Hovem, A.K. 1996. FORMEL: A Step Forward in Strength Logging. Colorado, USA.

Borba,. M. A., Ferreira, H. F., Santos, R. S. E. et al. 2014. UCS Estimation through Uniaxial Compressive Test, Scratch Test and Based Log Empirical Correlation. Goiania, Brazil.

York, P., Pritchard, D., Dodson, K. J. and Dodson, T. 2009. Eliminating Non-Productive Time Associated With Drilling Trouble Zones. Texas, USA.

Han, D., Batzle, M. and Liu, J. 2006. Acoustic Property of Heavy Oil – Measured Data. Annual Meeting, New Orleans.

Wang, Z., Nur, A.M., and Batzle, M.L. 1990. Acoustic Velocities in Petroleum Oils. J Pet technology 42 (2): 192-200. SPE-18163-PA.

Hashin, Z., and Shtrikman, S. 1963. A variational approach to the theory of the elastic behaviour of multiphase materials. J. Mech. Phys. Solids 11.

Edlmann, K., Somerville, J.M., Smart, B.G.D., Hamiltono, S.A., Crawford, B.R. 1998. Predicting Rock Mechanical Properties from Wireline Porosities. Trondheim, Norway. SPE 47344

Farquhar, R.A., Somerville, J.M., and Smart, B.G.D. 1994. Porosity as a Geomechanical Indicator: An Application of Core and Log Data and Rock Mechanics. London, UK. SPE 28853

Odunlami, T., Soroush, H., Kalathingal, P., and Somerville, J. 2011. Log-Based Rock Property Evaluation - A New Capability in a Specialized Log Data Management Platform. SPE. doi:10.2118/149050-MS

Sarda, J.P., Wicquart. E., Hannaford. K., and Deflander, J.P. 1993 Use of Porosity as a Strength Indicator for Sand Production Evaluation. Houston, Texas, 3-6 October. SPE 26454

Moos, D., Zoback, D.M., and Bailey, L. 1999. Feasibility Study of the Stability of Openhole Multilaterals. Cook Inlet, Alaska. Oklahoma, USA.

Rahman, K., Khaskar, A., and Kayes, T. 2010. An Integrated Geomechanical and Passive Sand-Control Approach to Minimizing Sanding Risk From Openhole and Case-and-Perforated Wells. Denver, USA.

Weingarten, J.S., and Perkins, T.K. 1995. Prediction of Sand Production in Gas Wells: Methods and Gulf of Mexico Case Studies.

Horsrud, P. 2001. Estimating Mechanical Properties of Shale From Empirical Correlations. SPE Drilling & Completion, June. SPE 56017

Buorgoyne, A.T., Millheim, K.K., Chenevert, E.M., and Young, F.S. 1986. Applied Drilling Engineering. USA. ISBN 1-55563-001-4

Carmichael, S.R. 1990. Practical Handbook of Physical Properties of Rocks and Minerals. Florida, USA. ISBN 0-8493-3703-8

Fjaer, E., Holt, M.R., Horsrud, P., Raaen, M.A., and Risnes, R. 2008. Petroleum Related Rock Mechanics, 2nd Edition. ISBN 978-0-444-50260

Mavko, G., Mukerji, R., and Dvorkin, J. 1998. The Rock Physics Handbook: Tools for Seismic Analysis in Porous Media. ISBN 0- 521-62068-6

Allen, B.M. 1987. BHA Lateral Vibrations: Case Studies and Evaluation of Important Parameters. New Orleans, USA. SPE/IADC 16110

Bailey, R.J. and Remmert, M.S. 2009. Managing Drilling Vibrations Through BHA Design Optimization. Doha, Qatar. IPTC 13349

Burgess, M.T., McDaniel, L.G., and Das, K.P. 1987. Improving BHA Tool Reliability With Drillstring Vibration Models: Field Experince and Limitations. New Orleans, USA. SPE 16109

Ramizer, S. and Aguilar, R. 2010. Evolution of Rotary Steerable BHA Designs in Mexico Offshore: Solution to Stop Multiple Drillstring Failures in High-Vibration Environment. Lima, Peru. SPE 138963

Chatar, C. and Blyth, M. 2011. Effective BHA Design and Vibration Modeling for Improving the Quality of Sonic Measurements. Amsterdam, the Netherlands. SPE/IADC 140326

Chen, K.C.D. 2007. Integrated BHA Modeling Delivers Optimal BHA Design. Cairo, Egypt. SPE/IADC 106935

Mason, S.J. and Sprawls, M.B. 1998. Addressing BHA Whirl: The Culprit in Mobile Bay. New Orleans, USA. SPE 52887

Payne, M.L. 1992. Drilling Bottom-Hole Assembly Dynamics. PhD Thesis. Texas, USA.

Nicholson, W.J. 1994. An Integrated Approach to Drilling Dynamics Planning, Identification, and Control. Dallas, USA.

Reckmann, H., Jogi, P., Kpetehoto, F., Chandrasekaran, S., and Macpherson, J. 2010. MWD Failure Rates Due to Driling Dynamics. New Orleans, USA. IADC/SPE 127413

Oueslati, H., Jain, R.J., Ledgerwood, L.W., and Pessier, R. 2013. New Insights Into Drilling Dynamics Through Hihg-Frequency Vibration Measurement and Modeling. New Orleans, USA. SPE 166212

Lake, W.L. 2007. Petroleum Engineering Handbook, Volume II. SPE. ISBN:978-1-55563-126-0

JPT staff, _. 1999. Downhole Dynamics Data Increases Drilling-Process Control. SPE. doi:10.2118/0299-0038-JPT

Lines, L. A., Mauldin, C. L., Hill, J. W., & Aiello, R. A. 2014. Advanced Drilling Dynamics Sensor Allows Real-Time Drilling Optimization, Damage Prevention and Condition Monitoring of RSS and LWD BHAs. SPE. doi:10.2118/170586-MS

Elsborg, C. C., & Grindhaug, G. 2006. Planning and Detailed BHA Vibration Modeling Lead to Performance Step Change Drilling Deviated 24-in. Hole Section, Offshore Norway. SPE. doi:10.2118/99126-MS

Fichter, L.S. 2000. A Basic Sedimentary Rock Classification. James Madison University, Virginia, USA.

Boggs, J.R. 2000. Principles of sedimentology and stratigraphy, 3rd edition. Toronto, Canada. ISBN 0-13-099696-3

Hood, J., Hovden, J., Heisig, G., Ernesti, K. D., and Knipper, A. 2003. Real-Time BHA Bending Information Reduces Risk when Drilling Hard Interbedded Formations. SPE. doi:10.2118/79918-MS

Bardet, J.P. 1997. Principles of Unconfined Compression Test. Prentice-Hall, New Yersey, USA.

Oueslati, H., Hohl, A., Makkar, N., Schwefe, T., & Herbig, C. 2014. The Need for High Frequency Vibration Measurement Along With Dynamics Modeling to Understand the Genesis of PDC Bit Damage. SPE. doi:10.2118/167993-MS

Jain, J. R., Oueslati, H., Hohl, A., Reckmann, H., Ledgerwood III, L. W., Tergeist, M., … Ostermeyer, G. P. 2014. High-Frequency Torsional Dynamics of Drilling Systems: An Analysis of the Bit-System Interaction. SPE. doi:10.2118/167968-MS

Pastusek, P. E., Sullivan, E., & Harris, T. M. 2007. Development and Utilization of a Bit Based Data Acquisition System in Hard Rock PDC Applications. SPE. doi:10.2118/105017-MS

Gegenhuber, N. 2016. Interpretation of Elastic Properties for Magmatic and Metamorphic Rock Types. International Journal of Rock Mechanics & Mining Sciences 88. http://dx.doi.org/10.1016/j.ijrmms.2016.07.007

Gegenhuber, N., Pupos, J. 2015. Rock Physics Template from Laboratory Data for Carbonates. Journal of Applied Geophysics 114.
http://dx.doi.org/10.1016/j.jappgeo.2015.01.005

Pettijohn, F.J. 1983. Sedimentary Rocks. Harpercollins, 3rd Ed.

Moore, C. H., Wade, J. W. 2013. Carbonate Reservoirs. Elsevier, 2nd Ed.

Ahr, M. W., 2008. Geology of carbonate Reservoirs: The Identification, Description, and Characterization of Hydrocarbon Reservoirs in Carbonate Rocks. John Wiley and Sons. DOI: 10.1002/9780470370650

Ehrenberg, S. N., & Nadeau, P. H. 2005. Sandstone vs. Carbonate petroleum reservoirs: A global perspective on porosity-depth and porosity-permeability Relationships. The AAPG Journal.

Mwanga, A., Rosenkranz, J., and Lamberg P. Testing of Ore Comminution Behaviour in the Geometallurgical Context – A Review. Minerals, 276-297. DOI: 10.3390/min5020276

Inglis, T.A. Petroleum engineering and development studies. Vol. 2: Directional drilling. USA. DOI: 10.1007/978-94-017-1270-5

Mihailović, K. 2002. Regresiona Analiza: objektivni pristup određivanja parametara funkcija. University of Belgrade, Belgrade.

Mitchell, R. F., & Samuel, G. R. (2007). How Good is the Torque-Drag Model? SPE. doi:10.2118/105068-MS

Mirhaj, A., Kaarstad, E., and Aadnoy, B. S. (2010). Minimizing Friction In Shallow Horizontal Wells. SPE. doi:10.2118/135812-MS

Gee, R., Hanley, C., Hussain, R., Canuel, L., and Martinez, J. (2015). Axial Oscillation Tools vs. SPE. doi:10.2118/173024-MS

Quigley, M. S., Dzialowski, A. K., and Zamora, M. (1990). A Full-Scale Wellbore Friction Simulator. SPE. doi:10.2118/19958-MS